ATOMIC RECOMBINATION IN A HYPERSONIC WIND TUNNEL NOZZLE

by

K. N. C. Bray,
Department of Aeronautical Engineering,
University of Southampton.

Thesis submitted for the Degree of
Doctor of Philosophy.

August, 1960.

CONTENTS

SUMMARY

The flow of an ideal dissociating gas through a nearly conical nozzle is considered. The equations of one-dimensional motion are solved numerically assuming a simple rate equation and a number of different values for the rate constant. These calculations suggest that deviations from chemical equilibrium will occur in the nozzle if the rate constant lies within a very wide range of values, and that, once such a deviation has begun the gas will very rapidly "freeze". The dissociation fraction will then remain almost constant if the flow is expanded further, or even if it passes through a constant area section. An approximate method of solution, making use of this property of sudden "freezing" of the flow, has been developed and applied to the problems of estimating the deviations from equilibrium under a wide range of conditions. If all the assumptions made in this paper are accepted, then lack of chemical equilibrium may be expected in the working sections of hypersonic wind tunnels and shock tubes. The shape of an optimum nozzle is derived in order to minimise this departure from equilibrium.

A comparison is made between the calculated results and data from shock tube experiments performed by Nagamatsu, Workman and Sheer at the General Electric Research Laboratory, using air as the test gas. Qualitative agreement is found.

It is shown from the calculations that, while the test section conditions are greatly affected by "freezing", the flow behind a normal shock wave is only changed slightly. The heat transfer rate

and drag of a blunt body are estimated to be reduced by only 25% even if complete freezing occurs. However, the shock wave shape is shown to be rather more sensitive to departures from equilibrium, and the flow past a slender body may be greatly affected.

LIST OF FIGURES

20. Pressure ratio versus temperature. Calculation for oxygen. $p_o' = 500$ p.s.i.

21. Pressure ratio versus temperature. Calculation for oxygen. $p_o' = 200$ p.s.i.

22. Pressure ratio versus temperature. Calculation for oxygen. $p_o' = 100$ p.s.i.

23. Pressure ratio versus temperature : effect of s. Calculation for oxygen. $p_o' = 500$ p.s.i.

24. Pressure ratio versus temperature : G. E. C. experiment on air. $p_o' = 500$ p.s.i.

25. Pressure ratio versus temperature : G. E. C. experiment on air. $p_o' = 200$ p.s.i.

26. Pressure ratio versus temperature : G. E. C. experiment on air. $p_o' = 100$ p.s.i.

27. Test section conditions.

28. Conditions behind a normal shock wave.

29. Mach angle and stand-off distance for a sphere.

30. Shock wave shapes for equilibrium and frozen flow (not to scale).

31. Some test section parameters affecting flow past a slender body.

SYMBOLS

a	=	reduced speed of sound
A	=	cross-sectional area of nozzle
B	=	$C\sqrt{\frac{A^x}{D/2m}}$
c	=	reduced characteristic speed : equation (24)
C	=	reaction rate constant defined in equation (16) : $(\text{Seconds})^{-1}$
D	=	dissociation energy per molecule
i	=	reduced specific enthalpy
k	=	Boltzmann's constant
k_D	=	dissociation rate constant (c.c. mole^{-1} sec.^{-1})
k_R	=	recombination rate constant (c.c.^{2} mole^{-2} sec^{-1})
K	=	constant in equation (36)
K_N	=	nozzle shape parameter related to expansion angle θ
m	=	mass of an atom
M	=	molecular weight
Mc	=	mach no. based on characteristic speed c
n	=	constant in equation (39)
N	=	number of steps with constant interval size in numerical integration
p	=	reduced pressure
q	=	stagnation point heat transfer rate
r	=	radius of a sphere
r_D	=	rate of dissociation : $(\text{seconds})^{-1}$
r_R	=	rate of recombination : $(\text{seconds})^{-1}$

R = radius of a spherical shock wave, also Reynolds number per unit length.

s = parameter in equation (16)

$\bar{S}$ = reduced specific entropy

T = reduced absolute temperature

t = time

u = reduced specific internal energy

v = reduced velocity

x' = axial distance from nozzle throat

Z = $x'/\sqrt{A'^{x}}$

α = ratio of mass of atoms dissociated to total mass of atoms and molecules

β = Mach angle : $\sin^{-1} c/v$

γ = ratio of specific heats

ε = maximum fractional error per step of integration.

Θ = half-angle of conical nozzle

$\textcircled{H}$ = constant in equation (39)

λ_o = initial interval size of step-by-step integration

Λ = a dissociation rate parameter (equation (49))

ξ = $\dfrac{K_N x'}{\sqrt{A'^{x}}}$ = dimensionless axial distance

ρ = reduced density

μ' = dimensional viscosity coefficient

Φ = $\dfrac{C}{2 K_N}\sqrt{\dfrac{A'^{x}}{D/2m}}$ = dissociation rate parameter

ψ = angle between local flow direction and a reference direction

$[\ ]$ = concentration in moles/c.c.

SUPERSCRIPTS

$(\ )'$ = dimensional quantity

$(\ )^{x}$ = quantity at a sonic throat

SUBSCRIPTS

d = characteristic dissociation quantity (equation 5)

e = equilibrium

f = frozen

t = test section

0 = stagnation

ot = pitot (pressure)

1 = ahead of normal shock wave

2 = behind normal shock wave

∞ = limiting value as $\zeta \rightarrow \infty$

Reduced quantities are formed by dividing dimensional quantities by the corresponding characteristic dissociation quantities.

1. INTRODUCTION

In attempting to simulate the conditions of high velocity flight it has become necessary to devise wind tunnels with very high stagnation enthalpies. Such facilities may vary widely in their mode of operation. Typical examples, in order of increasing stagnation temperature, are: tunnels with storage heaters, Smelt (1955), tunnels with piston-type compression heaters, Cox and Winter (1957), shock tube wind tunnels, Hertzberg (1957), and electric arc discharge tunnels, Lukasiewicz (1958). All these tunnels have in common the fact that they produce a high velocity flow by expanding the gas through a nozzle; this converts the thermal energy of random molecular motion into directed kinetic energy of the high speed flow. The amount of energy required is very large, so the temperature of the unexpanded gas must be high, and this means that the vibrational energy modes of the molecules will be excited to high levels, and the gas will be partially dissociated and perhaps ionised.

The flow through the nozzle is hypersonic, and so the rate of fall of temperature following the gas through the nozzle may be very large. As the temperature falls a wide variety of internal adjustments must continually be made by means of molecular collisions. The energy level of molecular vibrations must be reduced, a new balance must be found between atoms and molecules, chemical reactions must take place between the different species present and ions must recombine to form neutral particles. All these adjustments require a large number of collisions between molecules before they can reach equilibrium. If the time to reach equilibrium is of the same order

of magnitude as the time for a typical molecule to pass through the nozzle, then departures from equilibrium are to be expected, which may modify the flow pattern.

These so-called relaxation effects can occur whenever the temperature changes so fast that the internal structure of the gas cannot keep pace; other examples of interest to aerodynamicists are the flow round the "shoulder" of a blunt body in hypersonic flight and the flow through a strong shock wave. The latter problem has received considerable attention both theoretically : Wood (1956), Evans (1956), Freeman (1958), and Duff (1958), and experimentally : Hertzberg (1957), Rose (1957), Byron (1957) and Mathews (1959). Many attempts have been made to deduce the rate constants for the various relaxation processes from shock wave experiments, and some degree of success has been achieved. However, there is still considerable uncertainty about some of the rates of reaction (particularly those for dissociation), and also about their variation with temperature.

Two conditions must be satisfied if the relaxation of a particular degree of freedom is to affect the flow through a nozzle: the relaxation time must be comparable in magnitude with the time for the flow to pass through the nozzle, and the change in energy associated with the relaxing mode must form a significant part of the total change of enthalpy of the gas. Heims (1958) has applied these conditions to the flow of oxygen through a nozzle. He concludes that vibrational relaxation effects will be small compared with dissociation effects because of the energy condition, even though the

relaxation times may be comparable at high temperatures. Byron (1957) has reached the same conclusion as a result of shock tube experiments.

Similar arguments suggest that effects of ionisation relaxation will also be small until the temperature becomes large enough for a significant amount of energy to be involved in ionisation. It therefore appears that the dissociation and recombination of oxygen and nitrogen molecules and the formation and dissociation of oxides of nitrogen will be the most important relaxation effects to be considered. The possibility of interactions between different molecular energy modes must be remembered, however.

The present work is concerned with only one type of relaxation. Its object is to estimate the effects of finite rates of molecular dissociation and recombination on the performance of hypersonic wind tunnel nozzles, and to establish a suitable criterion for the conditions under which these rates will be important. The ideal dissociating gas of Lighthill (1957) and Freeman (1958), which is discussed in detail in the next Section, is used throughout. This simplified model of the gas behaviour cannot be expected to give accurate quantitative results in the present application, but it does represent the main features of a dissociating gas with sufficient simplicity to allow the problem to be formulated.

It is hoped that the criterion for equilibrium which is deduced here may later be applied to more accurate calculations, involving real gas properties.

The equations for the quasi-one-dimensional frictionless adiabatic flow of an ideal dissociating gas have been set up and solved for a number of different values of the reaction rate parameter. From these calculations it is deduced that the flow through a nozzle will "freeze" under certain conditions, when the rate of recombination of atoms to form molecules is too small to maintain equilibrium. Calculations have been made only for the wind tunnel case, in which flow is accelerated from rest through a convergent-divergent nozzle. However, the problem of the hypersonic shock tube, in which an already supersonic flow is expanded through a divergent nozzle, is also discussed, and it is shown that relaxation effects will be exactly the same as in the wind tunnel case, if the reaction rate parameter is greater than a certain value.

At temperatures for which dissociation is important, the rate of loss of heat from a gas by radiation is believed to be large. However, the energy radiated per unit mass of gas is a very strong function of the gas temperature, so that most of this radiation will take place in the stagnation region ahead of the nozzle throat, where the temperature is highest. Radiation is therefore neglected in the following calculations, it being assumed that the stagnation enthalpy has been reduced by an appropriate amount to allow for losses in the stagnation region.

No allowance is made for viscous effects, although these also are known to be very large in hypersonic nozzles. However, it seems reasonable to hope that there will be an inviscid core of flow in a real nozzle, for which an effective area ratio may be defined,

and to which the one-dimensional adiabatic flow equations will apply. Also, the rate equations near the walls will be greatly modified by the possibility of collisions between atoms or molecules and the walls; for this reason recombination is likely to be much more rapid near the walls, but these recombined molecules can only diffuse out from the walls at a finite rate, so they can only affect the flow within the boundary layer. The central core of adiabatic flow will be unaffected.

Because hypersonic nozzles employ small expansion angles, and also because boundary layer effects are known to be so large, reducing the effective expansion angle still further, a quasi-one-dimensional flow theory should be sufficiently accurate for the present purpose. The extra complication involved in allowing for velocity components normal to the nozzle axis does not appear to be justified at this stage.

Relaxation phenomena in nozzles have been studied by Penner (1955), Logan (1957), Heims (1958), Emmons (1958), Hall and Russo (1959) and many others. Penner, together with co-workers, has derived linearised theories for flow close to dissociation equilibrium and flows which are nearly frozen in their initial composition. From these he has derived simple criteria to determine the equilibrium state of the exhaust gases from a rocket nozzle. Logan (1957) applies a similar method to atomic recombination in a hypersonic wind tunnel. He assumes that departure from equilibrium will occur in regions where the rate of change of temperature is large, and uses the results of Penner (1955) which were derived for flow in rocket nozzles. He

takes the criterion:

$$\frac{1}{T}\frac{dT}{dt}\tau_{max} \leqslant 10^{-3}$$

for the flow to be near equilibrium. Here T is the actual value of the local temperature dT/dt is the rate of change of temperature with respect to time, and τ_{max} is the maximum value of the reaction time for the chemical process, that is the time to reach a value $(1 - \frac{1}{e})$ times the equilibrium concentration. On the basis of this criterion, Logan predicts large departures from equilibrium in a hypersonic wind tunnel nozzle where the rate of cooling can be very high. The lack of equilibrium is predicted to occur in the early part of the nozzle where dT/dt is large. This so-called "frozen" flow region is followed by an adjustment zone where equilibrium is regained by a sudden irreversible release of the dissociation energy, with a large increase of entropy, and an even larger decrease in the Mach number.

The present calculations suggest that, once an appreciable deviation from dissociation equilibrium has occurred in a hypersonic nozzle, a return to equilibrium is unlikely to take place within the nozzle. This must be compared with Logan's assumption that the region of partially frozen flow is followed by another zone in which full equilibrium is achieved.

These conflicting results may be understood when it is realised that the conditions in a rocket nozzle, with an area ratio of three or four, are very different from those in a hypersonic nozzle, which may have an area ratio of several thousand. The fall of density is therefore several orders of magnitude greater in the

wind tunnel nozzle than in the rocket case, and this has a large effect on the rate of atomic recombination, which requires a three body collision process and so depends on the density squared. It follows that an equilibrium criterion giving good results in the rocket nozzle case, where the density change is not large, will not be suitable for application to the nozzle of a hypersonic wind tunnel, without suitable modification to allow for the effects of density changes.

Since this work was first reported, Bray (1958), calculations by other authors, for example, Freeman (1958a), Hall and Russo (1959), have confirmed its main conclusions. Also, a certain amount of experimental work has been published on non-equilibrium nozzle flows : Wegener (1960), Nagamatsu, Workman and Sheer (1960), Lezberg and Lancashire (1960), and this also has tended to confirm the theoretical predictions. The present work contains a comparison between theoretical predictions for an ideal dissociating gas and the experimental results of Nagamatsu, Workman and Sheer (1960) for air.

2. THE IDEAL DISSOCIATING GAS

The thermodynamic changes in a real gas at high temperatures are extremely complicated, and not very well understood in detail. In order that gas dynamic theories may be at all general in application, it is necessary to find simple equations which will describe the changes of state of all gases with reasonable accuracy, within a specified range of temperatures and pressures. The ideal dissociating gas of Lighthill (1957) does just this, within the range of conditions where dissociation is the dominant effect.

If a partially dissociated gas, in conditions of thermal equilibrium, be regarded as a mixture of two perfect gases, the diatomic molecules and the atoms, then the equation of state for the mixture may be written

$$p' = \frac{k}{2m} \rho' T' (1 + \alpha) \qquad \ldots\ldots(1)$$

where p' is the pressure, ρ' the density, T' the temperature, α the ratio by mass of atoms dissociated to total of atoms and molecules; k is Boltzmann's constant and m is the mass of an atom.

The law of mass action, which determines the equilibrium composition of the mixture of atoms and molecules is (for a perfect gas)

$$\frac{\alpha^2}{1-\alpha} = \frac{\rho_d'}{\rho'} e^{-D/kT'} \qquad \ldots\ldots(2)$$

where ρ_d' is a characteristic density, a complicated function of the temperature. Lighthill shows that it is reasonable approximation to take ρ_d' = constant over a wide range of temperatures for both

oxygen and nitrogen. This greatly simplifies the problem; it is consistent with taking the vibrational degrees of freedom of the molecules as always being half-excited, even at low temperatures, and leads to the expression

$$u' = \frac{3k}{2m} T' + \frac{D}{2m} \alpha \qquad \ldots\ldots(3)$$

for the internal energy per unit mass, where D is the energy of dissociation. The specific enthalpy is then given by

$$i' = u' + \frac{p'}{\rho'} = (4+\alpha) T' \frac{k}{2m} + \frac{D}{2m} \alpha \qquad \ldots\ldots(4)$$

It will be seen that, as α approaches zero at low temperature, the ideal dissociating gas becomes a perfect gas with constant specific heats and with $\gamma = {}^{C_p}/_{C_v} = {}^{4}/_{3}$. This incorrect low temperature behaviour sets a lower limit below which air cannot be accurately represented by an ideal dissociating gas. An upper limit will also be fixed by the fact that electronic contributions to internal energy are neglected, as is ionisation.

Lighthill sets these lower and upper limits at approximately $3000^{\circ}K$ and $7000^{\circ}K$ for oxygen and nitrogen with densities between 10^{-3} and 1 of N.T.P. However, the ideal dissociating gas may be expected to show trends correctly over a much wider range of conditions, and if necessary corrections can be made at high and low temperatures. At low temperature, the rate of change of temperature with area ratio in a one-dimensional flow will be too small, because γ is too small. Neglecting electronic excitation and ionisation will make the calculated

temperature too high for very hot gases, because the electronic contributions to internal energy and ionisation energy have not been allowed for in full.

Following Lighthill, we define a characteristic temperature, density, pressure, internal energy and velocity for the gas (values of these quantities for oxygen and nitrogen are given in Table 1) :

$$\left.\begin{aligned} T_d' &= D/k \\ \rho_d' &= \text{a constant : Lighthill (1957)} \\ p_d' &= \rho_d' \, D/2m \\ u_d' &= D/2m \\ V_d' &= \sqrt{D/2m} \end{aligned}\right\} \quad \ldots\ldots(5)$$

TABLE 1

Characteristic Dissociation Quantities for Oxygen and Nitrogen

Lighthill (1957)

Quantity	Units	Oxygen	Nitrogen
T_d'	^{o}K	59,000	113,000
ρ_d'	gm/cm^3	150	130
p_d'	atm.	2.3×10^7	4.1×10^7
i_d'	k.cal/gm	3.67	8.02
V_d'	km/sec	3.9	5.8

and write equations (1), (2), (3) and (4) in terms of the dimensionless quantities T, ρ, p, u using T_d', ρ_d', p_d' and u_d' as units.

$$p = \rho T(1+\alpha) \qquad \ldots\ldots(6)$$

$$\frac{\alpha^2}{1-\alpha} = \frac{1}{\rho} e^{-1/T} \qquad \ldots\ldots(7)$$

$$u = 3T + \alpha \qquad \ldots\ldots(8)$$

$$i = (4+\alpha)T + \alpha \qquad \ldots\ldots(9)$$

These equations completely specify the thermodynamic behaviour of the ideal dissociating gas in equilibrium.

Lighthill's equilibrium theory may be extended to cases where equilibrium is not achieved, and for this purpose simple collision theory may be used. We consider the dissociation of unspecified diatomic molecules, represented by U_2, into free atoms represented by U, as well as the inverse recombination process. The two reactions considered are

$$U_2 + U_2 \underset{k_{R1}}{\overset{k_{D1}}{\rightleftharpoons}} 2U + U_2$$

$$U_2 + U \underset{k_{R2}}{\overset{k_{D2}}{\rightleftharpoons}} 2U + U$$

in which a molecule and an atom respectively act as the unchanged particle whose collision with the reacting particles brings about the reaction. Radiative recombinations and reactions involving other elements or compounds are neglected.

Then the rate constants that control the reactions are defined by the equation

$$\frac{d[U_2]}{dt} = -k_{D1}[U_2]^2 - k_{D2}[U][U_2] + k_{R1}[U]^2[U_2] + k_{R2}[U]^3 \qquad \ldots\ldots(10)$$

where the bracketed quantities are the concentrations in moles/c.c. of the various species. The rate constants obey the equation

$$K_e = \frac{k_{D1}}{k_{R1}} = \frac{k_{D2}}{k_{R2}} \qquad \ldots\ldots(11)$$

where K_e is the equilibrium constant which is given by

$$K_e = \frac{\rho_d'}{M} e^{-D/kT'} \qquad \ldots\ldots(12)$$

for the ideal dissociating gas, and M is the molecular weight of U_2. In terms of the dissociation fraction α, the molecule and atom concentrations are

$$[U_2] = (1-\alpha)\frac{\rho'}{M} \qquad \ldots\ldots(13)$$

and

$$[U] = \frac{2\alpha\rho'}{M} \qquad \ldots\ldots(14)$$

so that using equations (11), (12), (13) and (14) equation (10) may be written

$$\frac{d\alpha}{dt} = 4\frac{k_{R1}}{M^2}\rho_d'\rho'\left[(1-\alpha)+2\alpha\frac{k_{R2}}{k_{R1}}\right]\left\{(1-\alpha)e^{-D/kT'} - \frac{\rho'\alpha^2}{\rho_d'}\right\} \qquad \ldots\ldots(15)$$

The recombination rate constants k_{R1} and k_{R2} are assumed to be functions of temperature only. The classical collision theory described, for example, by Fowler and Guggenheim (1939), suggests that

each will be proportional to $(T')^{-s}$, where $s = \frac{1}{2}n - 1$ and n is the number of classical degrees of freedom of the two colliding particles which change their energy levels during the dissociation process. Suitable numerical values for s are discussed below.

A non-equilibrium theory for the ideal dissociating gas was first put forward by Freeman (1958), who argued that the variation with α of the numerical value of the term in the square bracket in equation (15) would not be large, since k_{R1} and k_{R2} are expected to be of the same order of magnitude. Freeman therefore neglected this α variation, assumed the same temperature dependence for k_{R1} and k_{R2}, and wrote

$$\frac{d\alpha}{dt} = C' \rho' (T')^{-s} \left\{ (1-\alpha) e^{-D/kT'} - \frac{\rho' \alpha^2}{\rho_d'} \right\}$$

where C' is assumed to be constant. We shall use this approximate rate equation because of its simplicity, but it will be written in the form :

$$\frac{d\alpha}{dt} = C \rho \left(\frac{T}{T_0}\right)^{-s} \left\{ (1-\alpha) e^{-1/T} - \alpha^2 \rho \right\} \qquad \ldots\ldots(16)$$

where C is a constant with dimensions $[\text{time}]^{-1}$.

This rate equation may not be accurate. Its derivation is based on simple collision theory which probably does not give a correct detailed picture of the reaction process. For example : Frood (1959) has argued that the net dissociation rate must depend on all the particles present and on all their energy states. Thus the existence of a small number of free electrons, or a few molecules with high rotational energy levels can have a large effect on the overall reaction

rate. Radiative recombination, which is a two-body process, may be important at low pressures but is neglected in equation (16); Zinman (1960) discusses this type of recombination very briefly. Also, the nozzle flows considered here involve very large changes in temperature, and so the experimental recombination rate data must be extrapolated over a wide temperature range, which may lead to errors. Even larger errors may arise if this rate equation is applied to the recombination of oxygen or nitrogen in air, because of the possibility of other recombination mechanisms involving, for example, nitrous oxide. This possibility is discussed briefly in a later section.

However, it is encouraging to note that the results of the numerical calculations which are described in this paper appear to be dominated by the term $e^{-1/T}$ in the dissociation rate for the upstream part of the nozzle; further downstream, where this rate has become small, the results are dominated by the ρ^2 term in the recombination rate. Both of these terms may be expected to occur in a more complicated rate equation, and this suggests that equation (16) may after all be adequate for our purpose, if the parameters C and s are suitably chosen for a limited range of conditions.

Some uncertainty still exists about the numerical values of C and s, although the situation has improved since this work was first published, Bray (1958). As explained above, s is related to the number n of classical degrees of freedom changing their energy during a dissociative collision. Freeman counts the relative translational energy of both particles but the rotational and vibrational energies of only one colliding molecule, on the grounds that the vibrational energies

are not fully excited and that molecules sometimes collide with atoms, and that a collision may not use all the available energy. This gives $\eta = 7$ and $s = 2.5$, which appears to be the maximum likely value of this parameter. Mathews (1959) assumes this value in interpreting the results of his shock tube experiments on Oxygen, but Byron (1957) deduces a value $\eta = 6$ ($s = 2$) from the results of similar shock tube experiments. Both authors stress the difficulty of assigning an exact value to this parameter. Other values have also been used : Wood (1956) takes $s = -\frac{1}{2}$, whereas the theoretical work of Wigner (1939) gives $s = \frac{1}{2}$. It is shown in the present paper that the value of s is not of paramount importance in the type of flow considered here, so $s = 0$ has been used for most of the calculations, though values between $-\frac{1}{2}$ and $2\frac{1}{2}$ have also been employed.

By comparing equations (15) and (16) it will be seen that

$$C = 4 \frac{k_{R1}}{M^2} \rho_d'^2 \left[(1-\alpha) + 2\alpha \frac{k_{R2}}{k_{R1}}\right] \left(\frac{T'}{T_0'}\right)^s \quad \ldots\ldots(17)$$

In order to calculate a value of C corresponding to the chosen value $s = 0$, we must therefore specify α, $\frac{k_{R2}}{k_{R1}}$ and also T', since k_{R1} is in general a function of temperature. The main dependence of C is of course on k_{R1}. Values chosen for oxygen were $\alpha = 0.5$ and $\frac{k_{R2}}{k_{R1}} = 3.5$ (an approximate value taken from the experiments of Byron, 1957). A summary of available data for oxygen is shown in Table 2, which was compiled from the paper by Mathews (1959). Values of C for $s = 0$ have been "matched" to the variable k_R data at two typical temperatures : 3000°K and 6000°K.

The rate constants of Byron and Mathews are from shock tube experiments, while those of Wigner and Logan are theoretical.

Table 2

Recombination Rate Data for Oxygen

Author	k_{R1} $cc^2 mole^{-2} sec^{-1}$	matched at 3000°K		matched at 6000°K	
		k_{R1}	$C\ (sec)^{-1}$	k_{R1}	$C\ (sec)^{-1}$
Byron (1957)	$9.2 \times 10^{19} T^{-3/2}$	5.6×10^{14}	1.9×10^{17}	2.0×10^{14}	6.7×10^{16}
Mathews (1959)	$6.0 \times 10^{23} T^{-5/2}$	1.2×10^{15}	4.1×10^{17}	2.1×10^{14}	7.2×10^{16}
Wigner (1939)	$1.9 \times 10^{17} T^{-1/2}$	3.2×10^{15}	1.1×10^{18}	2.3×10^{15}	7.8×10^{17}
Logan (1957)	3.6×10^{15}	3.6×10^{15}	1.2×10^{18}	3.6×10^{15}	1.2×10^{18}

These values are slightly different from those quoted previously, Bray (1959), because a more accurate allowance has been made for $\frac{k_{R2}}{k_{R1}}$. Also, the rate constant used by Wood (1956) is believed now to be much too small because he assumed $s = -\frac{1}{2}$, while that of Heims (1958), using the method of Wigner (1939), is believed now to be in error, and a corrected value is given by Mathews (1959). Probably the most accurate data available for oxygen is that of Mathews, giving C the values 4.1×10^{17} per second if matched at 3000°K, or 7.2×10^{16} per second if matched at 6000°K. It is worth noting that Byron (1957) found that the rate constant for oxygen dissociation was not greatly affected by the presence of nitrogen.

Data for nitrogen dissociation and recombination is more scanty at present, but shock tube experiments quoted by Kivel (1960)

indicate rates of the same order as those for oxygen.

If nitrogen and oxygen are present together, as in air, then many other chemical reactions are possible, and it may be that the value of C will have to be modified. This problem is discussed briefly in Section 7.

3. QUASI-ONE-DIMENSIONAL FLOW EQUATIONS

The frictionless adiabatic flow of an ideal dissociating gas through a duct of slowly varying cross-sectional area A' is described by the equations of conservation of mass, momentum and energy:

$$\rho v A' = \rho^* v^* A'^* \qquad \text{.....(18)}$$

$$v \frac{dv}{dx'} + \frac{1}{\rho} \frac{dp}{dx'} = 0 \qquad \text{.....(19)}$$

$$i + \tfrac{1}{2} v^2 = i_o \qquad \text{.....(20)}$$

together with the thermodynamic relationships of equations (6) and (9), which still apply if we assume that the atom and molecule temperatures are equal

$$p = \rho T (1 + \alpha)$$

$$i = (4 + \alpha) T + \alpha$$

and the rate equation (equation 16)

$$\frac{d\alpha}{dt} = c \rho \left(\frac{T}{T_o}\right)^{-s} \left\{ (1-\alpha) e^{-1/T} - \alpha^2 \rho \right\}$$

where quantities at a sonic throat are denoted by $(\quad)^*$, and i_o is the stagnation enthalpy, which is constant for adiabatic flow. The equations are written in terms of the dimensionless quantities which were introduced in equation (5).

The momentum and continuity equations may be written in terms of a reduced sound speed a which is defined in the usual way as $\left(\dfrac{dp/dx'}{d\rho/dx'} \right)^{1/2}$

so that

$$a^2 = \frac{T}{3}(4+\alpha)(1+\alpha) - \frac{d\alpha/dx'}{d\rho/dx'}\frac{\rho}{3}(1+\alpha-3T) \qquad .....(21)$$

and from equations (18) and (19)

$$\frac{1}{A'}\frac{dA'}{dx'} = \frac{1}{\rho v^2}\frac{dp}{dx'}\left(1-\frac{v^2}{a^2}\right) \qquad .....(22)$$

This shows that a is the velocity at which the stream tube area is a minimum, that is, the velocity at a "sonic throat" as in normal one-dimensional flow theory. Note that a depends not only on the variables of state but also on their derivatives (equation 21). However, equation (22) may be rewritten

$$\frac{1}{A'}\frac{dA'}{dx'} = \frac{1}{\rho v^2}\frac{dp}{dx'}\left(1-\frac{v^2}{c^2}\right) - \frac{d\alpha}{dx'}\left[\frac{1+\alpha}{3c^2} - \frac{3}{(1+\alpha)(4+\alpha)}\right] \qquad ....(23)$$

in terms of a reduced velocity c defined by

$$c^2 = \frac{T}{3}(4+\alpha)(1+\alpha) \qquad .....(24)$$

clearly, c depends only on variables of state and not on their derivatives. Equation (23) shows that c is the velocity at which dp/dx' cannot be obtained from the continuity and momentum equations. This is important for the one-dimensional flow calculations which follow, because it means that the critical point which in conventional flow through a convergent - divergent nozzle occurs at the sonic throat where $v = a$, will now occur at another point away from the throat, where $v = c$.

The velocity c is also important in the theory of characteristics for relaxing gases : Boa-Teh Chu (1957), Resler (1957),

and Clarke (1960). The equations of two-dimensional steady flow in streamline coordinates may be reduced to four simultaneous partial differential equations in the velocity v, its direction ψ, the pressure p and the dissociation fraction α. Four characteristic directions may be found for this system of equations. Two of these turn out to be coincident with the streamline direction, while the other two are at angles to the streamline direction given by

$$\pm \left[\frac{c^2}{v^2 - c^2} \right]^{1/2}$$

so that c rather than a is the velocity component normal to characteristic directions. The equations of motion along these two directions become the pair of ordinary differential equations

$$\frac{\delta \psi}{\delta \sigma} = \mp \left(\frac{v^2}{c^2} - 1 \right)^{1/2} \frac{1}{\rho v^2} \frac{\delta p}{\delta \sigma}$$

$$\mp \frac{\rho f c}{p v^2} \left\{ \frac{1+\alpha}{4+\alpha} - \frac{p}{\rho} \frac{3}{(4+\alpha)(1+\alpha)} \right\} \qquad \ldots\ldots(25)$$

where $\frac{\delta}{\delta \sigma}$ means differentiation along one of the characteristic directions defined above, and f is the rate function given in equation (16). The momentum and rate of dissociation equations apply as ordinary differential equations along the other characteristic direction (the streamlines). This system of equations can be solved by the usual numerical methods (Appleton, 1960).

Boa-Teh Chu (1957) has explained in detail the difference between the velocities a and c. He has shown that for a disturbance propagating in a gas mixture close to equilibrium, c is the velocity of propagation of the wave front while a is the velocity of the bulk of the disturbance. This result is relevant to section 8 of the

present paper, which discusses the effects of lack of equilibrium in a wind tunnel nozzle on various quantities which can be measured in the test section of the tunnel. One of the quantities considered is the angle to the flow direction formed by a weak wave, which is shown to be very sensitive to the amount of freezing in the nozzle, and the question arises as to whether such a wave propagates with velocity a or c. It is shown however that the numerical difference between these quantities is likely to be small under typical conditions.

Equations (6), (9), (16), (18), (19) and (20) cannot be solved until the nozzle shape is specified, so that $\frac{d\alpha}{dt}$ in equation (16) may be written in terms of $\frac{dA}{dA'}$. Many hypersonic wind tunnel nozzles at the present time are axi-symmetric, with a conical contraction and expansion, joined by a cylindrical throat. This throat shape is not suitable for theoretical study as the sharp corners between the conical and cylindrical parts lead to discontinuities in the theoretical flow, which will in practice be smoothed out by boundary layer effects. In order to obtain a valid solution through the throat, a nozzle with the hyperbolic area distribution :

$$A' = A'^{*} + K_N^2 x'^2$$

was chosen for these calculations, where x' is the axial distance from the throat and K_N is a constant. It will be seen that, at large distances from the throat, the nozzle becomes indistinguishable from a cone with half angle θ, where

$$\theta = \tan^{-1} \frac{K_N}{\sqrt{\pi}}$$

We proceed to define an area ratio $A = A'/A'^{*}$

and a dimensionless axial distance

$$\xi = \frac{K_N x'}{\sqrt{A'^{x}}}$$

so that the nozzle shape becomes

$$A = 1 + \xi^2 \qquad \text{.....(26)}$$

The system of seven equations, (6), (9), (16), (18), (19), (20), (26), may then be reduced to two simultaneous differential equations in α and i, with ξ as independent variable. These are

$$\frac{d\alpha}{d\xi}\left[1 - \frac{3(i-\alpha)}{(1+\alpha)(4+\alpha)}\right] + \frac{di}{d\xi}\left[\frac{6i_o}{1+\alpha} - \frac{7+\alpha}{1+\alpha}i + \alpha\right] + \frac{2\xi(i-\alpha)}{1+\xi^2} = 0$$

$$\frac{d\alpha}{d\xi} = \frac{\Phi \rho^x v^x T_o^s \left(\frac{4+\alpha}{i-\alpha}\right)^s}{(1+\xi^2)(i_o - i)}\left\{(1-\alpha)\, e^{-\frac{4+\alpha}{i-\alpha}} - \frac{\alpha^2 \rho^x v^x}{(1+\xi^2)\sqrt{2(i_o-i)}}\right\} \qquad \text{.....(27)}$$

$$\text{.....(28)}$$

where $\Phi = \frac{C}{2K_N}\sqrt{\frac{A'^{x}}{D/2m}}$ is a dimensionless dissociation rate parameter which contains the linear dimensions of the nozzle and its expansion angle as well as the chemical properties of the gas. It may be written approximately in the alternative form

$$\Phi = x'_t \frac{C}{2}\sqrt{\frac{2m}{D A_t}} \qquad \text{.....(29)}$$

where x'_t is the dimensional length of the nozzle and A_t is its exit area ratio.

As pointed out above, some uncertainty still exists about the value of the quantity C. The experimental results of Mathews

(1959) have been used to estimate the order of magnitude of Φ for oxygen, and the results are shown in figure 1, for various nozzle lengths and area ratios. The two sets of results have been obtained by matching Mathews' variable k_R data to our own $s = 0$ assumption at temperatures of 3000°K and 6000°K. Also marked on this figure are the nozzle lengths of the Southampton University hypersonic gun tunnel (Bray, Pennelegion and East (1958)), and the 50 inch "Hotshot" tunnel at A.E.D.C., Tullahoma (Lukasiewicz (1958)), which may be taken as typical of large and small installations.

It will be seen that the range of interest for Φ lies roughly between 3×10^{10} (Southampton tunnel, large area ratio, high matching temperature) and 3×10^{13} (50 inch "Hotshot" tunnel, small area ratio, low matching temperature). However, it must be remembered that the experimental data on recombination rates is not yet as accurate as one could wish, and that these limits may have to be modified.

The differential equations (27) and (28) which describe the relaxing one-dimensional flow of an ideal dissociating gas, cannot be solved analytically in general. However, in the limiting case of a gas for which $\Phi = 0$, that is, one for which the net rate of dissociation is negligibly small (frozen flow), equation (28) shows that the dissociation fraction α remains constant at its value at the entrance to the nozzle (α_0). Equation (27) can then be integrated to give:

$$\pm \ln(1+\xi^2) = -G \ln \frac{i-\alpha_0}{i_0-i} - \frac{1}{4}\frac{7+\alpha_0}{1+\alpha_0} \ln\left\{(i-\alpha_0)(i_0-i)\right\}$$

$$+ \text{constant} \qquad \ldots\ldots(30)$$

where $G = \frac{1}{2(i_o - \alpha_o)}\left[\frac{6 i_o}{1+\alpha_o} + \alpha_o - \frac{1}{2}(i_o + \alpha_o)\frac{7+\alpha_o}{1+\alpha_o}\right]$

The constant is determined from conditions at a sonic throat, where $\xi = 0$ by definition and

$$i^x = \frac{1+\alpha_o}{7+\alpha_o}\left[\alpha_o + \frac{6 i_o}{1+\alpha_o}\right]$$

from equation (27), so that $\left(di/d\xi\right)^x$ shall not be zero. It may also be derived from equations (20) and (21).

Equations (6), (8) and (9) show that the frozen gas will behave as a perfect gas with constant specific heats and a ratio of specific heats equal to $\frac{4+\alpha_o}{3}$. Thus, all the standard equations for the one-dimensional flow of a perfect gas may be used in this case.

The other limiting case, in which the reaction rate is so fast that equilibrium is reached everywhere in the flow, is given by letting Φ approach infinity in equation (28). Then, either

$$\frac{d\alpha}{d\xi} \to \infty \qquad \text{or} \qquad (1-\alpha)\, e^{-\frac{4+\alpha}{i-\alpha}} = \frac{\alpha^2 \rho^x v^x}{(1+\xi^2)\sqrt{2(i_o - i)}}$$

The latter is the law of mass action (equation (7)) for equilibrium. Together with the condition that the flow is isentropic, it yields the equation :

$$3 \ln T + \frac{1+\alpha}{T} + \alpha + 2 \ln \frac{\alpha}{1-\alpha} = \text{constant.} \qquad \ldots\ldots(31)$$

Hence, from the flow equations (18), (19) and (20), an expression for $d\alpha/d\xi$ may be deduced :

$$\frac{d\alpha}{d\xi} = \frac{\xi}{1+\xi^2} \frac{A(\alpha,T)}{B(\alpha)T^3 + C(\alpha)T^2 + D(\alpha)T - E(\alpha)} \qquad \ldots\ldots(32)$$

where $A(\alpha,T) = 4\alpha T(1+\alpha-3T)(1-\alpha)(i_0 - i)$

$B(\alpha) = (7+\alpha)(4+\alpha)(2-\alpha) - 3\alpha(1-\alpha)$

$C(\alpha) = 2\alpha(1-\alpha)(1+\alpha) - 6(2-\alpha)(i_0 - \alpha)$

$D(\alpha) = 3\alpha(1-\alpha)(3+\alpha)$

$E(\alpha) = 2\alpha(1-\alpha)(i_0 - \alpha)$

and $i = (4+\alpha)T + \alpha$

Equation (32) shows that $\frac{d\alpha}{d\xi} \to 0$ as $\xi \to 0$ unless

$$B(\alpha^*)T^{*3} + C(\alpha^*)T^{*2} + D(\alpha^*)T^* - E(\alpha^*) = 0 \qquad \ldots\ldots(33)$$

and this therefore yields a relation between α^* and T^* at a sonic throat. A simultaneous solution of this and equation (31) gives α^* and T^*. The mass flow rate $\rho^* v^*$ follows from equations (7), (9) and (20). Finally, for every equilibrium condition satisfying equation (31) a value of ξ can be found from the continuity equation (18)

$$\rho v(1+\xi^2) = \rho^* v^*$$

and the equilibrium flow can be solved.

Conditions a long way upstream of the throat ($\xi \to -\infty$) can be studied by expanding α, T, ρ, p, i and v as power series in $A^{-\frac{1}{2}}$ and substituting in equations (6), (9), (18), (19), (20), (16) and (26). From this it can be shown that the flow in this region is independent of Φ, to the order A^{-2}, so long as Φ is not identically zero. In other words, the solution to equations (27) and

(28) for this region is the equilibrium solution, independent of Φ. This is also to be expected physically, of course, since the velocity is small far upstream of the throat.

4. EXACT SOLUTIONS

Solutions of the differential equations (27) and (28) have been found numerically by a step-by-step procedure, for one set of stagnation conditions and a number of different values of the rate parameters Φ and S.

The method of solution for the smaller values of Φ was to start integration at equilibrium at a point well upstream of the throat where $\alpha \simeq \alpha_0$ and $i \simeq i_0$, and to seek by trial and error for a mass flow rate $\rho^* v^*$ which satisfied the condition $v = c$ at the critical point just downstream of the throat. Having determined $\rho^* v^*$ with the required accuracy, the solution was extrapolated through the critical point, using a graphical method in the (α, i) plane, in which the required solution is close to a straight line. A straight line extrapolation of the upstream solution was therefore drawn to intersect the line:

$$6(i_0 - i) = (i - \alpha)(1 + \alpha)$$

which is the locus of points for which $v = c$. The numerical integration was then continued from a point downstream of this intersection. Computations of this type were performed on the AMOS digital computer at A.R.D.E., Fort Halstead.

Fortunately, this lengthy and probably inaccurate trial and error procedure turned out not to be necessary in the majority of cases. For values of Φ greater than about 10^9, the flow was found to be still essentially in equilibrium at the critical point, and so the step-by-step integration was started from equilibrium in these

cases, at a point just downstream of the critical point. The equilibrium value of $\rho^{x} v^{x}$ was used. It was found that the exact initial point for these integrations did not materially affect the solution further downstream; a suitable means of choosing the initial point will be discussed in the next section. However, the interval size had to be very small in order to prevent the step-by-step integration from diverging, and so the computing times were long, especially for the larger values of Φ. To reduce this time to a minimum a new computational programme was devised for the Southampton University "Pegasus" which periodically chose the largest possible interval satisfying the condition that the integration error had to be less than a specified amount. The programme worked in the following way :

1. One step of integration was taken from an initial point ξ_1 with interval size λ_0 (a specified number) and the results were stored.
2. Two steps of integration were taken from the same point ξ_1, with interval size $\lambda_0/2$, and the results were stored.
3. If the fractional errors in these two calculated values of α and i at $\xi = \xi_1 + \lambda_0$ were less than a specified quantity ε, then $\lambda_0/2$ was chosen as the step size.
4. If the fractional error in either α or i was greater than ε, then two steps were taken from ξ_1, with interval $\lambda_0/4$, and the results were compared with those after one step with interval $\lambda_0/2$. This process was continued until the fractional error in both α and i was less than ε.

5. It will be seen that the maximum interval size which the programme could choose was $\lambda_o/2$, and this was often about 10^6 times greater than the initial interval size actually chosen near the critical point. Thus during the computation to choose the optimum interval size, integration was often performed with an interval size which was orders of magnitude too large. Under these conditions the integration often "blew up", so that the machine tried to take the square root or the logarithm of a negative number. It was arranged that each time this occurred, the interval size was automatically divided by a factor of two.

6. The computation to choose the interval size λ was automatically repeated after each set of N steps of integration.

It was found by experience that satisfactory results were obtained with the following values :

$$\lambda_o = 0.4$$

$$\varepsilon = 10^{-6}$$

$$N = 50$$

The stagnation conditions considered were $T_o = 0.1$ and $p_o = 5 \times 10^{-6}$; equivalent dimensional values of these and the other stagnation quantities for oxygen and nitrogen are given in Table 3.

TABLE 3

Stagnation Conditions for Oxygen and Nitrogen

Quantity	Units	Oxygen	Nitrogen
T_0'	^oK	5,900	11,300
ρ_0'	gm/cm^3	4.44×10^{-3}	3.84×10^{-3}
p_0'	atm.	115	205
i_0'	k.cal/gm	4.25	9.29
α_0	—	0.6899	0.6899

It will be remembered from the previous Section that Φ probably lies within the range

$$3 \times 10^{10} \leq \Phi \leq 3 \times 10^{13}$$

Some of the results of these calculations are shown in Figs. 2 to 9. The dissociation fraction α is plotted against the nozzle area ratio A in Fig. 2, for the limiting cases of frozen flow ($\Phi = 0$) and equilibrium flow ($\Phi = \infty$), and for three intermediate cases :

$\Phi = 3 \times 10^{9}$ (Southampton University tunnel, Wood's rate constant for oxygen : Wood (1956), now believed to be much too small);

$\Phi = 3 \times 10^{10}$ (Southampton University tunnel, Mathews' rate constant for oxygen, matched at 6000°K) and $\Phi = 3 \times 10^{12}$ (50 inch "Hotshot" tunnel, Mathews' rate constant for oxygen, matched at 3000°K). The parameter s is taken to be zero throughout. The intermediate solutions start off indistinguishable from the equilibrium case in the

upstream part of the nozzle, as predicted in the previous Section; but once a significant departure from equilibrium has begun, α very soon approaches a constant value, and does not change further, no matter how large A may become. This behaviour also is to be expected from the form of the rate equation (16), which in the downstream part of the nozzle is dominated by the recombination term, so that

$$\frac{d\alpha}{d\xi} \simeq -2\Phi\rho^2\left(\frac{T}{T_0}\right)^{-s}\frac{\alpha^2}{v}$$

The density is becoming very small in this region (see figure 3), and so $\frac{d\alpha}{d\xi}$ must become small also; in fact the velocity is almost constant at its limiting value, so that $\frac{d\alpha}{d\xi}$ approaches zero roughly as A^{-2} if $s = 0$. Once the flow has become frozen in this manner, equation (16) suggests that there is no chance of it unfreezing again further down the nozzle unless s is very large. Note that this behaviour is a direct result of the three-body collision process which is required for recombination; if recombination takes place in this way, then the ρ^2 term will always occur, whatever the details of the recombination equation. Presumably $\frac{d\alpha}{d\xi}$ will always become small if the density is sufficiently low.

Figs. 3, 4 and 5 show respectively the dimensionless density, velocity and temperature plotted against the area ratio for the cases $\Phi = 0$, 3×10^{10} and infinity, with $s = 0$. As before, the intermediate solution starts off from equilibrium and then quite suddenly diverges towards the frozen solution. The solutions for other values of Φ are not shown on these graphs as they behave in an

exactly similar manner; the case with $\Phi = 10^6$ is hardly distinguishable from frozen flow. The ratio of the characteristic speed c of equation (24) to the sound speed a (equation (21)) has been calculated for the same cases, and is shown in fig. 6; for equilibrium flow this ratio remains nearly constant, while for frozen flow it is always unity. The intermediate case drops sharply from the equilibrium curve as freezing occurs. Fig. 6 shows that the maximum error in using c instead of a is always less than 13% for the cases considered, and will be almost zero in the test section after freezing has occurred. Because this error is small, c rather than a has been used to define a Mach no. $M_c = V/c$, and this is shown in fig. 7. Freezing causes a large increase in Mach number, because of the fall in temperature.

The rate of change of the dimensionless specific entropy, $\bar{S} = \bar{S}'/\frac{k}{am}$ is given, Clarke (1960), by

$$\frac{d\bar{S}}{d\xi} = -\frac{d\alpha}{d\xi} \ln\left\{\frac{\alpha^2}{\alpha_e^2}\,\frac{1-\alpha_e^2}{1-\alpha^2}\right\}$$

where α_e here means the value α would take if the gas were allowed to reach equilibrium at the local values of T and p. This equation shows that the flow will be isentropic if the dissociation reaction is frozen so that $\frac{d\alpha}{d\xi} = 0$, and also if the reaction is in equilibrium so that $\alpha = \alpha_e$. Otherwise, there will be an entropy rise due to departure from equilibrium. This increase in entropy has been calculated from the results above, for the case where $\Phi = 3 \times 10^{10}$, and is shown plotted against A in fig. 8. It will be noted that the entropy rise is confined to the region where the flow is relaxing and

that the overall increase in dimensionless specific entropy is quite moderate, approximately 0.2. This is of the same order of magnitude as the entropy rise through a normal shock wave in the region where the flow is freezing, but much less than the entropy rise through a normal shock wave in the hypersonic part of the flow.

Integrations have also been carried out with various non-zero values of the parameter s, and figure 9 shows the variation of α with A when s takes the extreme value of 2.5, with the same stagnation conditions as were considered previously. It will be seen that the gas behaviour is qualitatively the same as for $s = 0$, with freezing taking place at the downstream end of the nozzle. However, the limiting value of α is somewhat smaller, and the approach to it is more gradual, as would be expected from the form of the rate equation. The effect of s upon the dissociation fraction is seen to be comparatively small.

Another feature of the calculations is that the flow at the nozzle throat ($\xi = 0$) is very nearly in equilibrium for all the cases considered, except for $\Phi = 0$ and 10^6. This means that the mass flow rate $\rho^* v^*$ is independent of Φ if Φ is sufficiently large. Actually, $\rho^* v^*$ does not vary greatly, even as $\Phi \to 0$; the limiting values are :-

$$\Phi = 0 \qquad \rho^* v^* = 0.868 \times 10^{-5}$$

$$\Phi = \infty \qquad \rho^* v^* = 0.797 \times 10^{-5}$$

Penner (1955) has considered the one-dimensional flow of reacting gas mixtures for application to propellant systems such as rocket engine nozzles. His fundamental equations are similar to the

equations of Sections 2 and 3, but he goes on to develop two linearised treatments for near-equilibrium and near-frozen flows. In the first of these he assumes that the temperature T in the relaxing flow is so close to the corresponding equilibrium temperature T_e that an effective equilibrium constant may be defined for the relaxing flow as the first two terms of a Taylor series expansion about T_e. This requires that

$$\frac{T_e - T}{T_e} << 1$$

Assuming that the approximation will become invalid if this fraction is greater than 0.5 then, if $A = 1000$, $T_0 = 0.1$ and $p_0 = 5 \times 10^{-6}$, we find that Φ must be greater than 2×10^{13}. Similarly, Penner gives a near-frozen solution, for which

$$\frac{T - T_f}{T_f} << 1$$

where T_f is the temperature for a given A with $\Phi = 0$. Assuming again that this fraction must be less than 0.5 we find, for the case quoted above, that Φ must be less than 3×10^{7}. It appears, therefore, that there may be a wide range of values of the rate parameter

$$3 \times 10^{7} < \Phi < 2 \times 10^{13}$$

in which these approximate solutions can give appreciable errors.

For the rocket nozzle case it may be permissible to neglect density changes in the nozzle when evaluating criteria for near-equilibrium and near-frozen flow (Penner (1955)), but this approximation is grossly in error in the case of a hypersonic wind tunnel, as figure 3 shows.

5. APPROXIMATE SOLUTIONS

The solutions of equations (27) and (28), which have been described in the last Section, all have the property that they are indistinguishable from the equilibrium solution (equations (31) and (32)) at points sufficiently far upstream. Fig. 2 shows that the larger the value of Φ the further downstream will the deviations from equilibrium occur, but that once such a deviation begins, α very soon reaches a constant value (α_∞). In other words the flow becomes frozen, and the rate equation is approximately

$$\frac{d\alpha}{dt} = 0$$

For convenience we will write the rate equation, equation (16), in the form

$$\frac{d\alpha}{dt} = \tau_D - \tau_R$$

where τ_D is the rate at which α is changing due to dissociation, and τ_R is the rate of change of α due to recombination, both evaluated while moving with the fluid. Three flow regions may then be distinguished :-

1) A region of flow near to equilibrium. Here both the rate of dissociation τ_D and the rate of recombination τ_R are very large in comparison with the net dissociation rate

$$\frac{d\alpha}{dt} = \tau_D - \tau_R$$

so the equilibrium condition $\tau_D = \tau_R$ is closely satisfied. Equilibrium will continue so long as this situation is maintained, that is so long as

$$-\frac{d\alpha}{dt} << \tau_D \qquad \text{.....(34)}$$

2) A transition region, in which ρ and T have fallen

sufficiently so that τ_D and τ_R are of the same order as $\frac{d\alpha}{dt}$, and there is consequently an appreciable departure from equilibrium. This results in an increase in the rate of fall of temperature, which reduces τ_D because of the exponential term and so increases the deviation from equilibrium. Once this process has begun, freezing takes place quite rapidly.

3) A region of almost frozen flow. Here the exponential decrease of τ_D has gone so far that this term is negligible

$$-\frac{d\alpha}{dt} >> \tau_D \qquad \ldots\ldots(35)$$

and consequently

$$-\frac{d\alpha}{dt} \simeq \tau_R$$

But τ_R is proportional to $\alpha^2 \rho^2$, if s is small, and so approaches zero faster than A^{-2}. The overall change of α in this region is small.

The two inequalities of equations (34) and (35) are the conditions for the gas to be near equilibrium and nearly frozen respectively. Freezing will take place suddenly if they are satisfied at adjacent points in the flow, and this will happen if τ_D is decreasing much more rapidly than τ_R as ξ increases. From the definitions of τ_D and τ_R, this means that $(1-\alpha)e^{-\frac{1}{T}}$ must approach zero faster than $\alpha^2\rho$, which is simply the condition that the gas shall not follow the law of mass action (equation (7)). Freezing reduces T and increases ρ, and the sudden nature of the change appears to be due to the exponential form in which T occurs in τ_D.

If the transition from equilibrium to frozen flow does take place within a small region of the nozzle, then it should be possible to construct an approximate solution of the flow problem, in which freezing is assumed to occur instantaneously at a particular point. The following is a simple attempt to define this point of sudden freezing.

Since $(-\frac{d\alpha}{dt})$ is much smaller than r_D for equilibrium and much larger than r_D when the flow has frozen, somewhere in the freezing region the two quantities must be of the same order of magnitude. We therefore write the following empirical equation for the point of sudden freezing :

$$-\frac{d\alpha}{dt} = K\, r_D$$

where K is an undetermined constant, which we would expect to be of order unity. Now up to this point the gas is assumed to be in complete equilibrium, so that $\frac{d\alpha}{dt}$ and r_D may be found from the equilibrium solution (equations (31) and (32)), and the equation for the freezing point becomes

$$-\left(\frac{d\alpha}{dt}\right)_e = K\, r_{De} \qquad \text{.....(36)}$$

where the suffix e denotes equilibrium. Equation (36) has been used to find the freezing point for the cases which were solved by step-by-step integration in the previous Section, and approximate solutions for the region downstream of the freezing point have been computed by setting $\Phi = 0$, so that equation (30) applies. The results of some of these calculations are compared with the more accurate integrations in Figs. 2, 4 and 5, from which it appears that

the approximation gives reasonable results in these cases. The constant K has been taken equal to unity; actually, better agreement with the more accurate calculations is obtained if K is 1.6, but the method probably does not warrant such accuracy, as K may actually vary. The results do not depend critically on the value chosen.

Equation (36) also gives the limiting value of the dissociation fraction as A goes to infinity (α_∞), and this is shown in figures 10 and 11, plotted against the rate parameter Φ for a wide range of stagnation conditions with $s = 0$. Figure 10 also gives the values of α_∞ determined from the numerical integrations of the previous Section and the results of two further numerical integrations at $T_o = 0.08$ and 0.12 to check the predicted temperature variation of α_∞. Once again, agreement with the approximate results is quite good. The variation of α_∞ with s is shown in figure 12; here the agreement between the approximate theory and the numerical integrations is not so good, suggesting that larger values of K are required for s greater than zero. The overall variation of α_∞ with s is shown to be small, but this does have a noticeable effect on the value of Φ required to maintain equilibrium, which may be decreased by a factor of about ten if s is changed from zero to 2.5.

It appears from Fig. 10 that if $s = 0$ the flow will be frozen everywhere if Φ is less than 10^6, approximately, and that it will be near to equilibrium everywhere if Φ is greater than a value Φ_e,

which varies from the region of 10^{14} with T_o = 0.07 to more than 10^{18} with T_o = 0.15. Anywhere within these very wide limits the gas will be partly frozen and partly in equilibrium. It follows that nozzle scale effects must be small, since Φ is directly proportional to the linear dimensions of the nozzle, and increasing the nozzle size by a factor of ten cannot reduce α_∞ by more than about 0.1 at the most, while the reduction may be very much less. Also we do not need to determine Φ very accurately, in order to estimate how much freezing will take place in a particular nozzle; this is fortunate in view of the present uncertainty about dissociation and recombination rates. Figs. 13 and 14 show the area ratio at which the sudden freezing of this approximate theory will occur, as a function of Φ, for various temperatures and pressures. Also indicated are values of Φ using the rate constant of Mathews (1959) for typical large and small nozzles. The intersections between the two sets of curves show the area ratios to which equilibrium may be maintained under various conditions.

The same results are plotted in a different form in figures 15 and 16. These show, as a function of stagnation temperature and pressure, the value of Φ required to reduce the frozen dissociation fraction α_∞ to one tenth of the stagnation enthalpy i_o. In other words, for the values of Φ shown in these figures, ten per cent of the energy supplied to the gas will be frozen in the form of uncombined atoms. The graphs also show dimensional values of the stagnation conditions for pure oxygen, and the required dimensional

nozzle lengths to give $\frac{\alpha_\infty}{i_o} = 0.1$, using Mathews' rate constant for oxygen (matched at 6,000°K) and assuming $A = 1000$. These results emphasise the enormous increase in nozzle size required to keep the gas close to equilibrium as T_o increases or p_o decreases. For example, figure 16 shows that, if p_o is reduced by a factor of 10, the nozzle length must be increased by about 10^5 if the fraction of energy frozen is to remain constant. Clearly, it will be very difficult to maintain equilibrium in low density high Mach number wind tunnels.

The above calculations have been concerned with the flow of a partly dissociated gas through a wind tunnel type of nozzle, in which gas initially at rest is accelerated to hypersonic speed through a convergent-divergent nozzle with a sonic throat. However, there is interest also in the case of the hypersonic shock tube. Here the air is accelerated to a low supersonic speed by the passage of a strong normal shock wave; it probably has time to reach thermodynamic equilibrium before it enters the divergent nozzle, and is accelerated to hypersonic speed. Under certain circumstances, then, the shock tube flow will be nearer to equilibrium than the corresponding wind tunnel flow. However, from the calculations above it appears that if Φ is sufficiently large the wind tunnel flow will also be in equilibrium at the point corresponding to the inlet of the shock tube nozzle, and the two flows will then be identical downstream. This will occur if Φ is greater than 10^{10}, approximately, for the cases considered here, with $p_o = 5 \times 10^{-6}$ and $s = 0$.

The criterion for the freezing point which was used above

(equation (36)) has since been checked experimentally by Wegener (1960), using a small supersonic wind tunnel, whose working fluid was nitrogen diluted by small percentages of NO_2 and N_2O_4. The stagnation conditions used were such that NO_2 molecules recombined to form N_2O_4 in the supersonic stream. It was found in these experiments that departure from equilibrium occurred in the manner predicted by equation (36), and the quantity K occurring in that equation was approximately constant and of order unity. Values of K determined from different experiments all lay within the range 0.42 to 1.25.

From the same experiments, Wegener deduced graphs of the quantities $\left|\frac{d\alpha}{dt}\right|$, τ_D and τ_R, plotted against distance down the nozzle, which showed very clearly the behaviour predicted at the beginning of this section.

This experimental evidence is encouraging, but it must be borne in mind that only the departure from equilibrium has been checked experimentally, not the sudden freezing approximation. The concept of sudden freezing can only be applied to nozzles with large area ratios, where the transition region defined at the beginning of this section forms a small part of the whole flow. Also, sudden freezing will only be a good approximation with gases for which τ_D falls rapidly as the temperature falls, so we require that s shall be small or negative. Again, the sudden freezing approximation can never be exact, because it does not take account of the entropy rise occurring in a real relaxing gas flow. However, the approximation is extremely simple to use, and appears to give quite a good

qualitative picture of relaxing gas flows.

Since this work was first published, Bray (1958), a similar sudden freezing analysis has been used by Hall and Russo (1959) employing a slightly different empirical criterion to find the sudden freezing point, and their method has been used to calculate the specific impulse of rocket nozzles (Hall, Eschenroeder and Klein (1960).

While the sudden freezing of this Section is empirical, and so open to question, there appears to be no doubt about the statement of equation (34) that a flow will be close to equilibrium if

$$\frac{\tau_{De}}{-\left(\frac{d\alpha}{dt}\right)_e} >> 1$$

and in fact this may be regarded as a definition of near equilibrium flow conditions, for any relaxation process. This concept has been used (Bray and Wilson (1960)) to study conditions under which a partly ionised argon plasma will depart from equilibrium. It was also used in the present work to choose a suitable starting point for some of the "exact" calculations of section 4. Trial integrations showed that if

$$\frac{\tau_{De}}{-\left(\frac{d\alpha}{dt}\right)_e} \geq 20$$

the flow was always sufficiently close to equilibrium so that integration could be started from local equilibrium conditions with negligible error.

6. EFFECTS OF NOZZLE SHAPE: THE OPTIMUM NOZZLE

Any conical nozzle is included in the above analysis, and the expansion angle does not appear explicitly in the results, as it is contained in the dimensionless rate parameter Φ. However, a wind tunnel working section is usually a duct of constant cross-sectional area, and this case needs special consideration.

We have shown in previous Sections that, if Φ lies within a certain wide range of values, the dissociation fraction α will approach a constant value α_∞ in the expanding part of the nozzle, and that the recombination rate $\left(-\frac{d\alpha}{dt}\right)$ will become small. In this Section we shall try to determine whether it is possible for $\left(-\frac{d\alpha}{dt}\right)$ to become larger again in a region of parallel flow, and hence whether α can deviate from α_∞ in such a region. We shall also consider the problem of finding an optimum nozzle shape, to avoid freezing as far as possible.

It is assumed that the transition to parallel flow takes place smoothly and in a short distance, so that the flow conditions at the beginning of the constant area region are the same as those at the end of the expansion. The rate equation (16) then shows that $\left(-\frac{d\alpha}{dt}\right)$ will be the same at both ends of this transition region. We wish to discover how rapidly $\left(-\frac{d\alpha}{dt}\right)$ can vary downstream of this point, and an upper limit to this variation is given by neglecting the rate of dissociation entirely, so that equation (16) becomes

$$-\frac{d\alpha}{dt} = C\rho^2\left(\frac{T}{T_o}\right)^{-s}\alpha^2$$

Now ρ is proportional to $\frac{1}{v}$, since the area is constant,

so if $s = 0$,

$$-\frac{d\alpha}{dt} \sim \left(\frac{\alpha}{v}\right)^2$$

The temperature is low in the working section, so equations (9) and (20) give

$$v^2 \simeq 2(i_o - \alpha)$$

and

$$-\frac{d\alpha}{dt} \sim \frac{\alpha^2}{i_o - \alpha}$$

This shows that $(-d\alpha/dt)$ gets smaller as α gets smaller; in fact, at the entrance to the constant area portion of the nozzle $(-d\alpha/dt)$ is already small, and it must become still smaller downstream, so there appears to be no likelihood of an appreciable change in α taking place within this region if $s = 0$. Putting $s = \frac{1}{2}$ multiplies all values of $d\alpha/dt$ in the above argument by a factor of about 5 for the cases considered in Section 4, but this is not nearly enough to affect the numerical value of α significantly.

It appears, then, that freezing will eventually take place in a nozzle of the type considered, and that a constant area working section of reasonable length will not unfreeze the gas appreciably. However, it is still possible that there is a different nozzle shape, which will give better results.

The maintenance of equilibrium in a nozzle depends not only on the rate constant of the gas passing through it, but also on the size and shape of the nozzle itself. These factors have been combined in the dimensionless rate parameter Φ , which determines whether the flow remains in equilibrium or how soon it freezes. For

conical nozzles Φ may be written in the form

$$\Phi = \mathcal{B} A^{1/2} \Big/ \frac{dA}{dz} \qquad \text{.....(37)}$$

where $\mathcal{B}$ is a reduced reaction rate constant $C\sqrt{\frac{A'^{*}}{D/2m}}$, and z is the ratio $x'/\sqrt{A'^{*}}$ where x' is the distance along the nozzle axis.

The area ratio at which sudden freezing will occur has been calculated from equation (36) as a function of Φ, for different stagnation conditions. The results are shown in Fig. 12. They enable us to estimate the minimum value of Φ required to expand a given flow through a given area ratio in a conical nozzle and maintain equilibrium. If the gas properties are known, equation (37) then gives the maximum allowable expansion angle for the nozzle. In practice this angle usually turns out to be very small, giving a conical nozzle which is much too long, and a test section flow which is filled by the wall boundary layer.

We therefore wish to find the shape of a nozzle which will expand the flow from a given throat area to a given test section area in the shortest possible length, consistent with the maintenance of thermal equilibrium, in order to cut down boundary layer growth. This will be called an optimum nozzle in the following paragraphs.

The optimum nozzle has a shape which keeps the flow continually on the verge of freezing, but never expands it quite fast enough for freezing to occur. Such a shape will clearly start with a large expansion angle near the throat where the temperature and

density are high so that the rate of recombination may be large, but the expansion angle will get progressively less further down the nozzle.

A very approximate expression for this shape may be found by regarding the optimum nozzle as being made up of a large number of conical sections, in each of which the expansion angle is chosen so that Φ is large enough to ensure equilibrium. Then, from equation (37), the optimum shape is given by

$$z = \frac{1}{B} \int_1^{A_t} \frac{\Phi(A)}{A^{1/2}} \, dA \qquad \ldots\ldots(38)$$

where $\Phi(A)$ is the rate parameter required to maintain equilibrium, which may be obtained from Figures 13 and 14. The equation of the corresponding conical nozzle, having the same value of Φ at its exit area A_t, and therefore giving the same test section conditions providing both nozzles do in fact maintain equilibrium, is

$$z = \frac{2}{B} \Phi(A_t) A^{1/2}$$

Now the data of Figures 13 and 14 is fitted quite well by an equation of the form

$$\Phi = (H) A^n \qquad \ldots\ldots(39)$$

where the constants (H) and n depend on the stagnation conditions. To this approximation the optimum nozzle shape, equation (38) becomes

$$z = \frac{(H)}{B} \frac{A^{n+\frac{1}{2}}}{n+\frac{1}{2}} \qquad \ldots\ldots(40)$$

and the ratio between the overall lengths of the conical and optimum

nozzles is simply

$$\frac{(z_t)_{con}}{(z_t)_{opt}} = 2n + 1 \qquad \ldots\ldots(41)$$

This ratio is plotted in Figure 17 against stagnation temperature, for the case $s = 0$. The variation with stagnation pressure is much less, as Figure 14 shows. It will be seen that the optimum nozzle is between one fifth and one tenth of the length of the corresponding conical nozzle, which should lead to a worthwhile saving in boundary layer growth.

An analysis of this kind is obviously not mathematically rigorous and so needs checking. In order to carry out such a check a few step-by-step integrations have been made for nozzles of the shape given in equation (40), with the parameters (H) and n taking the values indicated from Figures 13, 14 and 17. The dissociation fraction α obtained from these calculations for three different stagnation temperatures is compared with the corresponding equilibrium solutions in Figure 18. It will be seen that a flow very close to equilibrium is achieved in each case. A numerical example of the size and shape of the optimum nozzle is given below for a typical case.

We consider a hypersonic wind tunnel with an area ratio of 1000. The working fluid is oxygen and the stagnation conditions are $T_o = 0.1$ and $p_o = 5 \times 10^{-6}$ (corresponding to 5900°K and 115 atmospheres).

Figures 10 and 13 suggest that to ensure complete equilibrium in the test section of this tunnel the Φ - value for its conical nozzle

would have to be about 10^{15}, if $s = 0$. Figure 1 then shows that the nozzle would need to be 630 metres long, if the rate constant of Mathews (1959) is used, matched at 3000°K; the corresponding optimum nozzle would be 126 metres long. If s takes the extreme value of 2.5 the required Φ might be reduced to about 10^{14}, so the lengths of the conical and optimum nozzles would be 63 metres and 12.6 metres respectively. An optimum nozzle for this case, with a test section area of two square metres, is drawn to scale in Figure 19. Its shape requires some modification near the throat, which adds slightly to the length.

Nozzles of this type might not be practical for aerodynamic reasons even if they were smaller. However, the calculations above do suggest that a modest decrease in dissociation fraction for a given nozzle length may be achieved by suitable contouring. The initial rate of expansion downstream of the throat must be as large as other considerations will allow, and then the rate of expansion must be progressively reduced further downstream.

7. COMPARISON WITH G.E.C. EXPERIMENTS ON AIR

It is shown in the Appendix that experiments on non-equilibrium nozzle flows must be carefully planned, because of the accumulation of errors in all the quantities which must be measured. Results presented in the Appendix suggest that this accumulation of errors depends very much on the set of quantities chosen for measurement. It is shown that, in an experiment to determine whether or not a given flow is close to equilibrium, a suitable set of measurements for the chosen conditions consists of p_0 , T_0 , p_{0t} (the pitot pressure) and p_t (the test section static pressure). All of these can be measured by techniques which have already been developed, and, for the case considered in the Appendix, a 1% error in each measurement leads to a 5.6% error in the whole experiment. This is probably acceptable.

The same set of measurements has, in effect, been used by Nagamatsu, Workman and Sheer (1960) in their experimental study of departures from equilibrium in the nozzle of their hypersonic shock tunnel at the General Electric Research Laboratory, Schenectady, N.Y., using air as the working fluid. For this, they first deduced the effective area ratio of their nozzle in low stagnation temperature flow from measurements of p_0 , p_{0t} and p_t . At higher stagnation temperatures where relaxation effects occurred they assumed that the nozzle effective area ratio was unchanged, and so studied the departure from equilibrium from measurements of three quantities: T_0 , p_0 and p_t . The simultaneous and accurate measurement of these quantities in a

short duration facility is believed by the present author to be a considerable achievement.

In order to compare these G.E.C. results with our own theoretical predictions, the equations of the previous sections have been solved for conditions corresponding to those used in the experiments. Results have been obtained for dimensionless stagnation pressures between 2.96×10^{-7} and 1.48×10^{-6}, dimensionless stagnation temperatures up to 0.15, area ratios of 144 and 56.2 and values of the dimensionless rate parameter Φ between 3×10^{10} and 3×10^{14}. The corresponding dimensional stagnation conditions for pure oxygen are pressures between 100 and 500 p.s.i.a. and temperatures up to 8000°K. The non-equilibrium cases were calculated by the approximate "sudden freezing" analysis of Section 5, and also in some cases by numerical integration (Section 4). A high-speed digital computer was used for all the calculations.

Results are presented in the form of graphs, (figs. 20, 21 and 22) of p_t/p_o plotted against T_o, for various values of Φ, p_o and θ_t. Of the non-equilibrium solutions, the full line curves have been calculated by the approximate method, with the constant K in equation 36 set equal to unity, the circled points have been obtained from "exact" solutions (i.e. by numerical integration), and the dashed curves in figures 20 and 21 are approximate solutions with K = 2.3. From these results it will be seen that the approximate "sudden freezing" solution with K = 1 predicts values of p_t/p_o which are consistently too low. Setting K = 2.3 gives good agreement with "exact" solutions for

$\Phi = 3 \times 10^{13}$ over a range of temperatures, but at larger values of Φ a K closer to unity is required. It is concluded that a suitable empirical choice of K can give a very good numerical fit to the "exact" solutions. "Sudden freezing" solutions with K = 1 do lead to appreciable errors, but appear to predict correctly the trend of variation of p_t/p_o with T_o, p_o and Φ.

Another parameter to be chosen is the temperature exponent s in equation 16. Figure 23 shows the effect of varying this between 2.5 and - 0.5 for $\Phi = 3 \times 10^{12}$. The effect on the overall shape of the curves is comparatively small.

Figures 24, 25 and 26 show the results of experiments on air taken from the work of Nagamatsu, Workman and Sheer (1960), for the same stagnation conditions and area ratios as those used for the calculated results shown in figures 20, 21 and 22. The experimental curves are plotted to the same scales as the corresponding calculated values.

It must be stressed that detailed numerical comparison between the theoretical and experimental curves is not possible, because of differences in the working fluid. The idea dissociating gas has larger variations in the local value of the ratio of specific heats than real air; firstly because at low temperature in equilibrium $\gamma \to 5/3$ instead of 1.4 as in air, and secondly because the ideal dissociating gas is assumed to be pure oxygen, whereas of course about 79% of air is nitrogen, which remains largely undissociated under these conditions. Consequently, the difference in pressure between the frozen and equilibrium limits is much less for air than it is for the ideal

dissociating gas.

However, there is a strong resemblance between the theoretical and experimental curves. This suggests that the simple mechanism for atomic recombination which is implied in equation (16), namely that recombination takes place as a result of triple collisions between two atoms and a third particle, is probably the dominant mechanism of the real recombination process in air.

On the basis of simple collision theory, and neglecting oxides of nitrogen, a rate equation for the dissociation and recombination of oxygen in air may be derived, in a manner similar to that employed in Section 2, in the form:-

$$\frac{d\alpha}{dt} = F(\alpha, \beta, c)\, c\, \frac{\rho'}{\rho_d'} \left\{ (1-\alpha) e^{-\frac{D}{kT'}} - \frac{\rho' c}{\rho_d'} \alpha^2 \right\} \qquad \cdots (42)$$

where $c\rho'$ is the total density of oxygen atoms and molecules, and $(1-c)\rho'$ is the total density of nitrogen; α is the density of oxygen atoms divided by the total oxygen density; β is the density of nitrogen atoms divided by the total nitrogen density, and

$$F(\alpha, \beta, c) = \frac{4 \rho_d'^2 k_{R1}}{M_{O_2}^2} \left[(1-\alpha) + 2\alpha \frac{k_{R2}}{k_{R1}} + \frac{1-c}{c}(1-\beta) \frac{M_{O_2}}{M_{N_2}} \frac{k_{R3}}{k_{R1}} + \frac{1-c}{c} 2\beta \frac{M_{O_2}}{M_{N_2}} \frac{k_{R4}}{k_{R1}} \right]$$

The first two terms in the square bracket are the same as those in equation (17), while the third and fourth terms represent recombinations in which a nitrogen molecule and a nitrogen atom respectively acts as the third body. The recombination rate constants k_{R3} and k_{R4} refer to these reactions and the quantities M_{O_2} and M_{N_2} are

molecular weights for oxygen and nitrogen. Equation (42) is very similar in form to equation (16) and in particular both give recombination rates proportional to (density)^2, because three-body collisions are assumed. On the other hand, a recombination mechanism involving "shuffling" reactions such as the formation of nitric oxide (see, for example, Zinman (1960)) could bring about recombination of atomic oxygen as a result of two-body collisions, and this would give a recombination rate directly proportional to density. This mechanism could lead to an increase in the rate of recombination in the downstream part of the nozzle where the density is low, and thus to a less sudden freezing.

Another effect which could lead to discrepancies between theory and experiment is boundary layer growth in the nozzle used for the G.E.C. experiments. It was assumed there that the nozzle effective area ratio was constant at a given station, whereas presumably the boundary layer thickness would tend to be greater at the larger stagnation temperatures. Any correction for this effect, if present, would tend to drop the high temperature part of the experimental curves towards the frozen limit, and so accentuate the experimental trend to frozen flow at high temperatures which is the chief difference between the experimental and theoretical curves. This difference might be reduced by taking a negative value of the temperature exponent s in equation (16), but shock tube experiments on oxygen, Byron (1957), suggest a positive value of s. A possible explanation of this discrepancy may be the presence of atomic nitrogen in the high temperature experiments.

It must be admitted, however, that the correspondence between

the theoretical and experimental working fluids is not sufficiently close to enable one to distinguish between these various possible effects. If a purely empirical fit is sought between the ideal dissociating gas calculations and the experimental results in air, by matching values of the ratio $\frac{p - p_f}{p_e - p_f}$ at a given T_o, it is found that values of Φ between 3×10^{12} and 3×10^{13} give the best agreement if $s = 0$. Figure 1 shows that these values are of the order of magnitude that would be predicted for the G.E.C. shock tunnel (length $x_t' = 52$ c.m.s.) with small area ratios, on the basis of the rate constant for oxygen determined by Mathews (1959) evaluated at 3000°K.

The results described in this Section have been published previously by Bray and Makin (1960).

8. EFFECTS OF LACK OF EQUILIBRIUM IN THE TEST SECTION

The calculations presented above suggest that the flow in the test section of a hypersonic wind tunnel may deviate considerably from chemical equilibrium for a wide range of stagnation conditions, and the G.E.C. experiments discussed in Section 7 confirm this conclusion. We must therefore consider what effects these non-equilibrium phenomena will have on quantities measured in the tunnel test section.

One effect will be that the test fluid will not have the correct thermodynamic and chemical properties for simulating real flight conditions, as it will contain too large a fraction of atoms. Quantities such as the local value of the ratio of specific heats will not be correctly reproduced, and any local departure from equilibrium in the flow past the body will also be greatly affected by freezing in the nozzle. On the other hand, if the aim of the experiment is to reproduce flight conditions at a great altitude where oxygen and nitrogen in the atmosphere are already partly dissociated, then freezing in the wind tunnel may in fact be an advantage. The data for the A.R.D.C. Model Atmosphere (Minzner, Champion and Pond, 1959) suggests that oxygen dissociation occurs at altitudes between 100 and 200 kilometers and the same publication shows that the mean free path in the atmosphere between these altitudes increases rapidly from 3 c.m. at 100 k.m. to 200 m. at 200 k.m. Thus, at altitudes where a large amount of atomic oxygen occurs, the flow past a vehicle will probably be close to free molecular, so that non-equilibrium nozzle flow will always provide a test gas with too large a dissociation fraction, except perhaps in

genuinely free molecule flow wind tunnels.

A second effect of departure from equilibrium in the nozzle flow is that test section conditions can no longer be deduced from measured stagnation conditions simply by assuming an isentropic expansion on a Mollier diagram using equilibrium gas properties. In fact, considerable errors can arise from this procedure, as illustrated by figure 27, which shows the conditions that will be encountered at an expansion ratio of 1000 with $s = 0$, $T_o = 0.1$ and $p_o = 5 \times 10^{-6}$, as calculated in Section 4, plotted against the rate parameter Φ. It will be seen that the velocity is slightly reduced by freezing and the density is correspondingly increased; however the temperature is reduced by a factor of about 40 and the static pressure by about 17. These large changes may be expected to have a considerable effect on the flow past bodies in the tunnel.

Many bodies at present being tested are more or less blunt-nosed and will therefore have nearly normal shock waves in front of them, so it is of interest to see what effect freezing in the flow upstream of a normal shock will have on the flow behind it. If conditions ahead of the shock are denoted by a suffix (1) and those behind by (2), then the conservation equations are:

$$\rho_1 V_1 = \rho_2 V_2 \qquad \ldots.(43)$$

$$p_1 + \rho_1 V_1^2 = p_2 + \rho_2 V_2^2 \qquad \ldots.(44)$$

$$i_1 + \tfrac{1}{2} V_1^2 = i_2 + \tfrac{1}{2} V_2^2 \qquad \ldots.(45)$$

The conditions ahead of the shock are known from the nozzle

calculations of Section 4 as functions of ξ or A, so the shock wave equations can be solved at a given ξ. It is assumed for the present that equilibrium is reached quickly behind the shock, so that

$$\frac{\alpha_2^2}{1-\alpha_2} = \frac{1}{\rho_2} e^{-1/T_2}$$

from the law of mass action (equation (7)). This is a reasonable assumption, as the high temperature and pressure behind the shock will favour rapid equilibrium; however, relaxation effects behind the shock are discussed later in this Section.

Using the thermodynamic relationships of Section 2 and neglecting p_1, which must be very much smaller than $\rho_1 V_1^2$ if the flow is hypersonic, equations (43), (44), and (45) may be written:

$$\frac{\rho^* v^*}{A_1} = \rho_2 v_2 \qquad \ldots\ldots(46)$$

$$\frac{\rho^* v^*}{A_1}\sqrt{2(i_0 - i_1)} = p_2 + \rho_2 v_2^2 \qquad \ldots\ldots(47)$$

$$i_0 = i_2 + \tfrac{1}{2} v_2^2 \qquad \ldots\ldots(48)$$

The left-hand sides of equations (46) and (48) are independent of nozzle relaxation effects, since we have shown that the mass flow $\rho^* v^*$ does not vary much with Φ. The left-hand side of equation (47) does contain i_1, which depends on Φ, but the numerical

variation of the whole term is not large. Also, from equation (48), the enthalpy behind the shock (i_2) cannot differ greatly from the stagnation enthalpy (i_0), since the velocity behind a strong shock wave is small, so that i_2 must be almost independent of Φ. It follows that the equilibrium conditions behind a normal shock wave in hypersonic flow cannot be greatly affected by relaxation in the nozzle upstream of the shock.

Solutions of equations (43), (44) and (45) have been found by Lighthill's iteration method (Lighthill (1957)) for the case with $S = 0$, $T_0 = 0.1$, $p_0 = 5 \times 10^{-6}$ and $A_1 = 1000$, by using the results of Section 4, and the results of these calculations are shown in Fig. 28. It will be seen that α_2 and T_2 are almost independent of the degree of freezing in the nozzle, but that freezing reduces the density behind the shock to about 75% of its equilibrium value. The pitot pressure, p_{02} is also shown in Fig. 28, and it also is reduced somewhat by freezing. To the accuracy of the Newtonian approximation, the pressure drag of a given body is proportional to the pitot pressure, so the p_{02} curve shows that pressure drag forces will be underestimated in a frozen flow. An estimate of the effect of non-equilibrium in the nozzle on the heat transfer rate at the stagnation point of a blunt body can also be made. Fay and Riddell (1958) have solved the heat transfer problem for a wide range of conditions; here their solution for equilibrium within the boundary layer has been used together with the assumption of constant wall conditions, and Fig. 28 shows the calculated ratio of heat transfer rate to heat transfer rate with $\Phi = 0$.

Freezing in the nozzle is seen to cause a reduction in the measured heat transfer rate.

Further, the simple blunt body theory described by Lighthill (1957), in which the flow between the shock wave and the nose of the body is assumed to be incompressible, can be applied to determine the stand-off distance of a shock wave in front of a spherical nose (see Fig. 29). The stand-off distance depends on the shock wave density ratio; ρ_2 is reduced by freezing while ρ_1 is increased, and the resulting change in ρ_2/ρ_1 is sufficient to increase the stand-off distance by a factor of two as the flow freezes.

According to approximations of the Newtonian type the shock wave in front of a blunt body closely follows the body shape near the front stagnation point. Further round the body the shock separates from the surface, and after this its strength gradually weakens and its inclination gradually approaches that of a Mach wave. It is therefore of interest to calculate the Mach angle

$$\beta = \sin^{-1} \frac{c}{V}$$

and this has been done from the calculations of Section 4. The results are shown in Fig. 29, from which it will be seen that the Mach angle is reduced by a factor of about three if freezing occurs, mainly because of the large fall in static temperature. This result, together with the increase in stand-off distance, suggests that a measurable change in shock wave shape may be expected as a result of nozzle freezing. This effect is illustrated in the sketches of Fig. 30, which are not to scale.

The above analysis of flow past a blunt body neglects any lack of equilibrium in the flow between the shock wave and the spherical nose, but Freeman (1958) has provided the necessary extension to non-equilibrium flows. He shows that for a given set of equilibrium conditions upstream of the shock, the stand-off distance depends on a dimensionless rate parameter

$$\Lambda = \frac{2r C T_o^s}{\sqrt{D/2m}} \frac{\rho_1}{v_1} \qquad \ldots.(49)$$

in our notation, where r is the radius of the sphere. The ratio of our rate parameter Φ to Freeman's Λ is

$$\frac{\Phi}{\Lambda} = \frac{\sqrt{A'^{K}}\, v_1}{4 K_N r T_o^s \rho_1}$$

Now for a typical model in a typical hypersonic wind tunnel, this ratio is of the order of $1/\rho_1$, (if $s = 0$), that is, about 10^8. But Freeman shows that most of the relaxation effects behind the shock wave occur, for a typical example, in the range

$$0 \leq \Lambda \leq 100$$

or approximately in the range

$$0 \leq \Phi \leq 10^{10}$$

The nozzle flow will still be nearly frozen with Φ in this range, so that as the gas passes through the shock α only has to make the small change from α_0 to α_2; this should reduce the effects of relaxation behind the shock. If $\Phi > 10^{10}$ so that the nozzle flow is approaching equilibrium, then $\Lambda > 10^2$ and relaxation behind the shock is again negligible in its effect on the

stand-off distance. It therefore seems reasonable to assume, as we did earlier in this Section, that the stand-off distance, as measured in a hypersonic wind tunnel, depends only on relaxation effects in the wind tunnel nozzle itself. However, Freeman's analysis could, if necessary, be modified to allow for a non-zero value of α_1.

A much longer calculation would enable one to estimate the required stagnation conditions, so that a non-equilibrium nozzle flow would correctly simulate given free flight conditions at the stagnation point of a blunt body. This analysis will not be attempted here. However, simple arguments indicate that in order to simulate the given conditions the non-equilibrium nozzle flow will require larger values of the stagnation temperature and stagnation pressure than a completely equilibrium nozzle flow giving the same conditions.

The simulation in a non-equilibrium nozzle flow of flight conditions other than at the front stagnation point of a blunt body is a much more difficult problem. If either the flow past the full size vehicle or the local flow past the wind tunnel model is relaxing, then exact simulation will in general be impossible. This is because the dissociation fraction α will vary between different limits in the two cases.

In the special case where the local flow past both the model and the full size vehicle is frozen, simulation will be achieved for many problems if the free stream Mach number, Reynolds number and ratio of specific heats are the same in the two cases.

It is therefore of interest to study the variation of these parameters as the nozzle flow changes between the limits of completely

equilibrium and completely frozen flow. The relevant Mach number for locally frozen flow is

$$M_c = v_t \sqrt{\frac{3}{(4+\alpha_t)(1+\alpha_t)T_t}}$$

and the free stream Reynolds number per unit length $R = \frac{\rho_t' v_t'}{\mu_t'}$ divided by its value R_f for completely frozen nozzle flow is

$$\frac{R}{R_f} = \frac{\rho_t v_t}{\rho_{tf} v_{tf}} \frac{\mu'_{tf}}{\mu'_t}$$

Since the mass flow rate is almost independent of freezing process in the nozzle, this reduces to μ'_{tf}/μ'_t and if we make the very simple approximation that $\mu' \sim T'$, which is in order of magnitude agreement with the data of Hansen (1958) even in the presence of considerable dissociation, then

$$\frac{R}{R_f} = \frac{T_{tf}}{T_t}$$

Finally, the ratio of specific heats for locally frozen flow is

$$\gamma = \frac{4+\alpha_t}{3}$$

Figure 31 shows the quantities M_c, $\frac{R}{R_f}$ and γ plotted against the rate parameter Φ for the same stagnation conditions as above, at an area ratio of 1000. It will be noted that the free stream Mach number and Reynolds number per unit length are greatly increased by freezing in the nozzle and the ratio of specific heats is also increased significantly.

It may be possible, by a more sophisticated analysis than the above, to correct experimental results for the effects of non-equilibrium

nozzle flows. Further work is required on this aspect of the problem.

9. CONCLUSIONS

If the assumptions which have been made in this paper are accurate, then the flow of a partly dissociated gas through a hypersonic shock tube or wind tunnel nozzle will remain in chemical equilibrium until a certain point in the nozzle is reached. Downstream of this point the gas will "freeze" quite rapidly, so that its composition will remain almost constant if the flow is expanded further or passed through a constant area test section. It is suggested that this behaviour is a consequence of the triple-body collision process through which recombination occurs, and that freezing can be avoided only if the reaction rate parameter Φ is greater than a value Φ_e. This is about 10^{15} for the typical case considered in Section 4, if the area ratio of the nozzle is 1000 and $s = 0$. Increasing the stagnation temperature or decreasing the stagnation pressure increases Φ_e, but a positive value of s decreases it. If s is increased from zero to 2.5, Φ_e is reduced by a factor of about ten.

The values of Φ achieved for the flow of oxygen in large and small nozzles with various values assumed for the rate constant are believed to lie within the range

$$3 \times 10^{10} \leq \Phi \leq 3 \times 10^{13}$$

so it is concluded that freezing will occur under conditions of practical interest, particularly at low stagnation pressures, high stagnation temperatures and large nozzle area ratios. Comparison of predicted static pressure variation for an ideal dissociating gas

with the results of experiments on air, carried out by Nagamatsu, Workman and Sheer (1960) at the General Electric Research Laboratory, shows qualitative agreement. An empirical recombination parameter obtained from this comparison is of the same order of magnitude as that obtained from the shock tube experiments of Mathews (1959) for oxygen.

The shape of an optimum nozzle has been derived in order to expand the gas in equilibrium in the shortest possible length. This is shown to be about one fifth of the length of the corresponding conical nozzle, but it is still too long for practical applications.

The flow near the nose of a blunt body in the tunnel test section is shown to be affected only slightly by freezing in the nozzle, but the shock wave shape may be altered significantly. Further work is required on the interpretation of experimental results obtained from models placed in non-equilibrium nozzle flows.

ACKNOWLEDGEMENTS

The author would like to express his sincere gratitude to all of the following:

To Professor E.J. Richards whose encouragement was a very real assistance in all phases of this work.

To the staffs of the Computation Departments of the Armaments Research and Development Establishment at Fort Halstead, and the University of Southampton, for their assistance with the numerical computations.

To Messrs. J.P. Appleton and B. Makin of the University of Southampton for valuable assistance with certain parts of this work.

To the Director, A.R.D.E., Fort Halstead, where the author was employed as a Vacation Consultant when the earlier part of this work was carried out.

To the Wright Air Development Division, Air Research and Development Command, United States Air Force, who have supported the more recent part of this work through their European Office, under Contract No. A.F.61-(052)-250.

REFERENCES

Appleton, J.P. (1960)	Univ. Southampton Aero. and Astro. Rep. No. 146.
Boa - Teh Chu (1957)	W.A.D.C. TN. 57-213.
Bray, K.N.C. (1958)	A.R.C. 19,983.
Bray, K.N.C. (1959)	J. Fluid Mech. 6, 1.
Bray, K.N.C. and Appleton, J.P. (1959).	Univ. Southampton, Aero. and Astro. Rep. No. 120.
Bray, K.N.C. and Makin, B. (1960).	Univ. Southampton Aero. and Astro. Rep. No. 143.
Bray, K.N.C., Pennelegion, L., and East, R.A. (1958)	A.R.C. 20,520.
Bray, K.N.C. and Wilson, J.A. (1960)	Univ. Southampton Aero. and Astro. Rep. No. 134.
Byron, S.R. (1957)	Cornell Univ. Ph.D. Thesis.
Camac, M., Camm. J, and Petty, C. (1958)	A.V.C.O., Res. Lab. Rep. 22.
Clarke, J.F. (1960)	J. Fluid Mech. 7, 4.
Cox, R.N. (1959)	Proc. Colston,Research Soc., University of Bristol, Butterworths, London.
Cox, R.N. and Winter, D.F.T. (1957)	A.G.A.R.D. Rep. No. 139.
Duff, R.E. (1958)	Physics of Fluids, 1, 3.
Emmons, H.W. (1958)	Heat Trans. and Fluid Mech. Inst. Univ. of California, Berkeley.
Evans, J.S. (1956)	N.A.C.A. TN. 3860.
Fay, J.A. and Riddell, F.R.	J. Aero. Sci. 25, 2.
Fowler, R.H. and Guggenheim, E.A. (1939)	Statistical Thermodynamics, Cambridge Univ., Press.
Freeman, N.C. (1958)	J. Fluid Mech. 4, 4.

Freeman, N.C. (1958a)	A.R.C. 20,340.
Frood, D.G.H. (1959)	A.R.C. 21,211.
Hall, J.G., Eschenroeder, A.Q. and Klein, J.J. (1960).	A.R.S. Journal 30, 2.
Hall, J.G., and Russo, A.L. (1959)	Cornell Aero. Lab. Rep. No. AD-1118-A-6.
Hansen, C.F. (1958)	N.A.C.A. TN. 4150.
Heims, S.P. (1958)	N.A.C.A. TN. 4144.
Hertzberg, A. (1957)	Cornell Aero. Lab. Rep. No. AD-1052-A-5.
Hoenig, S.A. (1959)	A.R.S. Journal 29, 5.
Kivel, B. (1960)	A.V.C.O. Res. Lab. Rep. AMP. 34.
Lezberg, E.A. and Lancashire, R.B. (1960)	Fourth A.G.A.R.D. Combustion and Propulsion Colloquium, Pergamon Press, London.
Lighthill, M.J. (1957)	J. Fluid Mech. 2, 1.
Logan, J.G. (1957)	I.A.S. Preprint No. 728.
Lukasiewicz, J. (1958)	Paper presented to 1st Int. Congress Aero. Sci. (Madrid).
Mathews, D.L. (1959)	Physics of Fluids 2, 2.
Minzer, R.A., Champion, K.S.W. and Pond, H.L. (1959)	U.S.A.F. Surveys in Geophysics, No. 115. (A.R.C. 21,810)
Nagamatsu, H.T., Workman, J.B. and Sheer, R.E. (1960)	General Electric Research Lab. Rep. No. 60-RL-2332C.
Penner, S.S. (1955)	Chemical Reactions in Flow Systems, Butterworths, London.
Resler, E.L. (1957)	J. Aero. Sci. 24, 11.
Rose, P.H. (1957)	A.V.C.O. Research Note 37.
Smelt, R. (1955)	Proc. Conf. on High Speed Aero., Poly. Inst. Brooklyn.

Wegener, P.P. (1960) A.R.S. Journal 30, 4.

Wigner, E.P. (1939) J. Chem. Phys. 7, 8.

Wood, G.P. (1956) N.A.C.A. TN. 3634.

Zinman (1960) A.R.S. Journal 30, 3.

APPENDIX

Choice of Measurements in an Experiment on Atomic Recombination

The calculations described in Sections 4 and 5 have given the flow conditions in a nozzle as a function of four quantities: p_o, T_o, A and Φ. Clearly, the flow properties may be expressed as a function of any four suitable independent variables, and so an experiment on a relaxing gas flow requires the measurement of four quantities in order to specify the thermodynamic and gas dynamic properties of the system completely. Any fifth measurable quantity may then be expressed as a function of these four.

Quantitative experimental studies of non-equilibrium gas flows may therefore be very difficult to perform accurately, because of the accumulation of experimental errors in all the quantities which must be measured. Such errors are likely to be large, because of the short duration and unsteady character of the flow in the shock tube wind tunnels which produce the very high temperatures necessary for these experiments.

This Appendix is concerned with the accuracy of experiments to determine whether a given flow is closer to the equilibrium or the frozen state. The work described here has been reported in greater detail elsewhere (Bray and Appleton 1959).

In order to determine whether a given flow is in equilibrium it is necessary to measure four quantities P, Q, R and S. We may then use P, Q and R to calculate two values of S; the first value S_e assumes that the flow is in complete equilibrium, and the second value S_f assumes the flow to be everywhere frozen. The actual state of the gas

is indicated by comparing these calculated values with the measured value S.

If δP, δQ, δR and δS are the errors in measuring P, Q, R and S then, assuming that the frozen and equilibrium flow calculations are accurate, the total error is given by

$$\Delta S = \delta S + \left[\left(\frac{\partial S_e}{\partial P}\right)_{QR} + \left(\frac{\partial S_f}{\partial P}\right)_{QR}\right]\delta P + \left[\left(\frac{\partial S_e}{\partial Q}\right)_{PR} + \left(\frac{\partial S_f}{\partial Q}\right)_{PR}\right]\delta Q + \left[\left(\frac{\partial S_e}{\partial R}\right)_{PQ} + \left(\frac{\partial S_f}{\partial R}\right)_{PQ}\right]\delta R$$

This total error must be much less than $|S_e - S_f|$ if the experiment is to be successful. We therefore define a fractional error for the experiment as a whole, given by

$$\frac{\Delta S}{|S_e - S_f|} = C_P \frac{\delta P}{P} + C_Q \frac{\delta Q}{Q} + C_R \frac{\delta R}{R} + C_S \frac{\delta S}{S} \qquad \text{---(A1)}$$

where

$$C_P = \frac{P}{|S_e - S_f|}\left[\left(\frac{\partial S_e}{\partial P}\right)_{QR} + \left(\frac{\partial S_f}{\partial P}\right)_{QR}\right]$$

$$C_Q = \frac{Q}{|S_e - S_f|}\left[\left(\frac{\partial S_e}{\partial Q}\right)_{PR} + \left(\frac{\partial S_f}{\partial Q}\right)_{PR}\right]$$

$$C_R = \frac{R}{|S_e - S_f|}\left[\left(\frac{\partial S_e}{\partial R}\right)_{PQ} + \left(\frac{\partial S_f}{\partial R}\right)_{PQ}\right]$$

$$C_S = \frac{S}{|S_e - S_f|}$$

In order that the experiment may be accurate we must carefully choose the measured quantities P, Q, R and S so that the coefficients in equation (A1) are small.

The results described in Sections 4 and 5 have been used to obtain numerical values for these coefficients for some typical sets of measurements. The quantities P, Q and R were selected from p_0, T_0, p_{0t} and v_t, and S was selected from p_t, ρ_t, T_t and α_t. Values of the coefficients are shown in Table 4 for a typical set of conditions ($p_0 = 5 \times 10^{-6}$, $T_0 = 0.1$ and $\Phi = 3 \times 10^{10}$, with A = 100 and 1000). It can readily be seen from this table that the coefficients vary very widely, the largest coefficient being $C_{v_t} = -1320$ in Case (11), where p_0, T_0 and v_t are the measured quantities corresponding to P, Q and R, ρ_t corresponds to S and A = 1000. This means that a 1% error in will lead to a 1320% error in the experiment. The smallest coefficient is $C_{p_0} = 0.0327$ in Case (1) where p_0, p_{0t}, v_t and T_t are measured at A = 1000.

Table 4 - Coefficients for Experiment 1. $P_o = 5 \times 10^{-6}$, $T_o = 0.1$, $\Phi = 3 \times 10^{10}$.

Case No.	A	P, Q, R				S				Σ
		C_{P_o}	C_{T_o}	$C_{P_{o_t}}$	C_{V_t}	C_{P_t}	C_{ρ_t}	C_{T_t}	C_{α_t}	
1	1000	-0.0327		0.112	0.336			0.121		0.601
	100	0.0834		0.168	-0.359			0.320		0.930
2	1000	0.133	-0.950	-0.0678				0.121		1.27
	100	0.123	-1.00	-0.0745				0.320		1.52
3	1000	0.0563		1.21	-1.32	0.177				2.77
	100	0.0875		1.63	-2.68	0.420				4.82
4	∞	-0.262	2.88	0					0.652	3.79
	1000	-0.336	3.71	-0.0716					0.742	4.86
	100	-0.448	4.97	-0.161					0.915	6.49
5	1000	0.367	-4.15	0.853		0.177				5.55
	100	0.388	-4.93	1.02		0.420				6.75
6	1000	-0.357		0.132	7.16				0.742	8.39
	100	-0.391		0.324	8.25				0.915	9.88
7	∞	-0.262	2.88		0				0.652	3.79
	1000	-0.593	6.97		-1.95				0.742	10.3
	100	-0.746	8.70		-2.11				0.915	12.5
8	1000	-0.254	6.32		-8.08			0.121		14.8
	100	-0.170	5.07		-6.50			0.320		12.1
9	1000	0.594	-10.6	5.10			2.24			38.6
	100	0.933	-16.5	7.20			3.16			27.8
10	1000	-1.49	22.8		-72.7	0.177				97.1
	100	-0.500	40.0		-52.0	0.420				85.9
11	1000	-20.0	804		-1320		2.24			2150
	100	-4.67	325		-495		3.16			828

Although Table 4 shows the coefficients to vary over a very wide range and also in a manner which seems at first sight to be somewhat haphazard, the variation is in a direction which may in fact be predicted. If we consider first the S variables, the coefficients are smallest when the variables are greatly affected by whether the flow is in the frozen or the equilibrium state; T_t and p_t are such variables. On the other hand, the coefficient associated with ρ_t is greater than unity since ρ_t is little affected by the equilibrium state of the gas; that is $|\rho_{te} - \rho_{tf}| < \rho_t$.

However, the variation in the coefficients of P, Q and R is much greater. These are large when two of the measured quantities (P and Q, say) are closely related, because then the partial derivatives $\left(\frac{\partial S}{\partial P}\right)_Q$ and $\left(\frac{\partial S}{\partial Q}\right)_P$ will be large. For example: the test section velocity v_t approaches the limiting velocity V_∞ as A becomes large, and this depends mainly on T_o. Cases 7, 8, 10 and 11 all show large coefficients because both v_t and T_o have been measured. Case 11 gives a double example of this effect since ρ_t is measured as well as v_t and T_o. Now the mass flow rate $\rho_t v_t A_t$ is almost unaffected by freezing, so that ρ_t and v_t are related, and again the coefficients are large. This is by far the worst case.

In the last column of Table 4 is shown a quantity Σ, defined as the sum of the moduli of the four coefficients. It is the maximum overall percentage error of the experiment for a one per cent error in each of the measured quantities, and so may be used as a rough criterion for the accuracy of the experiment. The eleven cases shown in Table 4 are listed in order of increasing Σ for an area ratio

of 1000; that is, the more accurate experiments are near the top of the list.

To get an order of magnitude for the maximum acceptable value of $\leq$ we may assume that a five per cent error is made in each of the four measured quantities. Then, for a maximum of thirty per cent error in the experiment, $\leq$ must be equal to six or less. Only the first five cases in Table 4 satisfy this criterion.

It is difficult to estimate the accuracy to be expected in the various measurements which are called for in this analysis. However, a rough classification may be attempted, according to the accuracy to be expected from measurements in a short duration, high enthalpy facility such as a hypersonic shock tube or gun tunnel. It is necessary to distinguish between the comparatively high temperature and high pressure conditions in the supersonic flow just downstream of the throat, and the much lower temperatures and pressures in the hypersonic flow further downstream, where many measurements are much more difficult to perform. The quantities to be measured are :-

p_o - can be measured accurately

p_{ot} - can be measured accurately in both supersonic and hypersonic flow

p_t - can be measured accurately in supersonic flow, but only inaccurately at present in hypersonic flow.

ρ_t - can be measured accurately in supersonic flow, but cannot at present be measured under hypersonic wind tunnel conditions because of lack of sensitivity

T_o - can probably be measured accurately by the spectrum line reversal method, but development is required. Can also be deduced with unknown accuracy from shock velocity measurements.

T_t - can probably be measured accurately in the hot supersonic part of the flow, by the spectrum line reversal method, but development is required. No satisfactory technique is known for the cold, hypersonic part of the flow.

V_t - can probably be measured accurately in the supersonic part of the flow, where the density is high enough for schlieren photography to be employed, in order to follow the path of a disturbance introduced into the flow (Cox, 1959). Development is required, and the method will probably not be applicable to the truly hypersonic part of a nozzle flow, where the density is too low for schlieren photography.

α_t - various techniques are under development (Camac, Camm and Petty (1958); Hoenig (1959)) which may be applicable to both supersonic and hypersonic flow conditions, but accurate measurements are not likely at present.

It is now possible to assess the various combinations of measurements which were considered above, in order to estimate which combination will lead to the most accurate experiment.

In Table 4 we placed them in order of increasing Σ for $A = 1000$. The best combinations are :-

Case 1 - (P_o, P_{ot}, v_t, T_t) Σ = 0.601

This involves two quantities, v_t and T_t, which at present can only be measured in the supersonic as opposed to hypersonic part of the nozzle. With this restriction all four measurements may be accurate, and the whole experiment should be satisfactory. At A = 100 a 5% error in each measurement leads to less than 5% overall error.

Case 2 - (P_o, T_o, P_{ot}, T_t) Σ = 1.27

Again T_t is required, and this can at present be measured only in the hot supersonic part of the nozzle. Also the T_o measurement requires further development for the gun tunnel. If a shock tube is used T_o may be deduced from shock velocity measurements, and the experiments should then lead to accurate results in the supersonic part of the flow.

Case 3 - (P_o, P_{ot}, v_t, P_t) Σ = 2.77

Measurement of v_t has been classified as supersonic only, because of the difficulty of obtaining schlieren photographs under low density hypersonic conditions. Also P_t has been classified as an inaccurate measurement for hypersonic flow. The experiment should be satisfactory for supersonic conditions.

Case 4 - $(P_o, T_o, P_{ot}, \alpha_t)$ Σ = 4.86

In contrast to the three cases above, none of the quantities in this set is restricted to the low supersonic region of the nozzle. The T_o measurement requires further development from the gun tunnel, but can probably be deduced quite accurately from the shock speed in a

conventional shock tube. Measurement of α_t requires development and may not be accurate.

Case 5 - (p_o, T_o, p_{ot}, p_t) Σ = 5.55

Of this set of measurements, p_o and p_{ot} should be accurate, and values of T_o deduced from shock speed measurements are probably satisfactory for the shock tube wind tunnel, but a technique for T_o is still required for the gun tunnel. Only p_t has been listed as inaccurate, and fortunately its coefficient is small and decreasing as A increases. None of these measurements is limited to the supersonic, as opposed to hypersonic, part of the flow. If p_o, T_o and p_{ot} are each measured with 5% error and p_t with 10% error, then the experiment may be 29% in error, which may be acceptable, as the object here is merely to determine whether or not the flow is close to equilibrium.

This is probably the most obvious set of measurements to make, as all the necessary techniques have already been developed, and reasonable accuracy appears possible. Experiments of this type have in fact been carried out in a shock tube wind tunnel at area ratios up to 144 by Nagamatsu, Workman and Sheer (1950), as described in Section 7.

The calculations reported here must be regarded as no more than an example, since only one set of stagnation conditions and one rate parameter are considered, and not all the possible combinations of measured quantities are included. Even with these restrictions the amount of calculation involved is considerable. However, it is

hoped that the work illustrates the importance of choosing the best set of quantities for measurement, not only in nozzle flow relaxation experiments, but also in other studies of non-equilibrium gas flows.

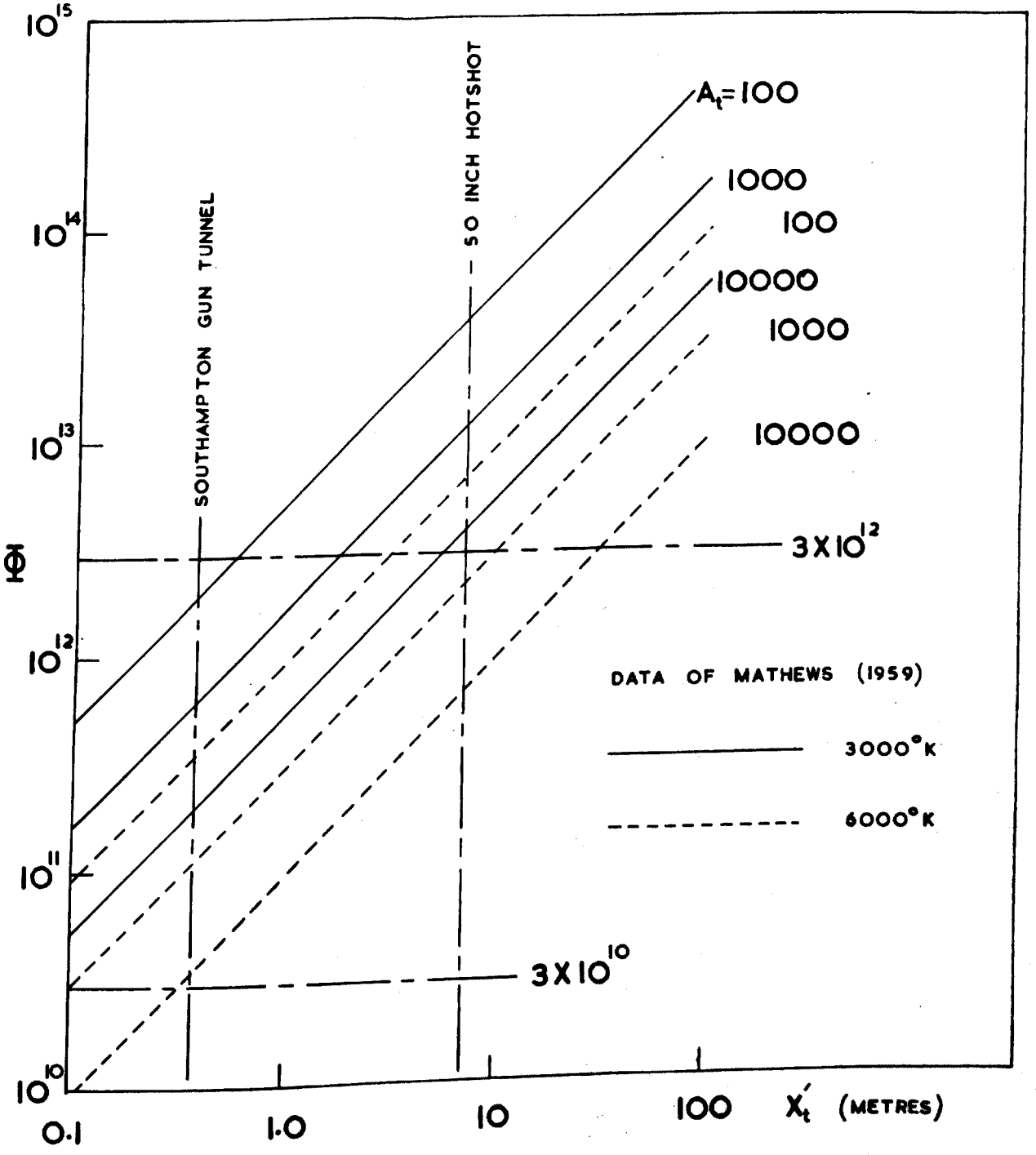

FIG.1 The dissociation rate parameter for oxygen in conical nozzles.

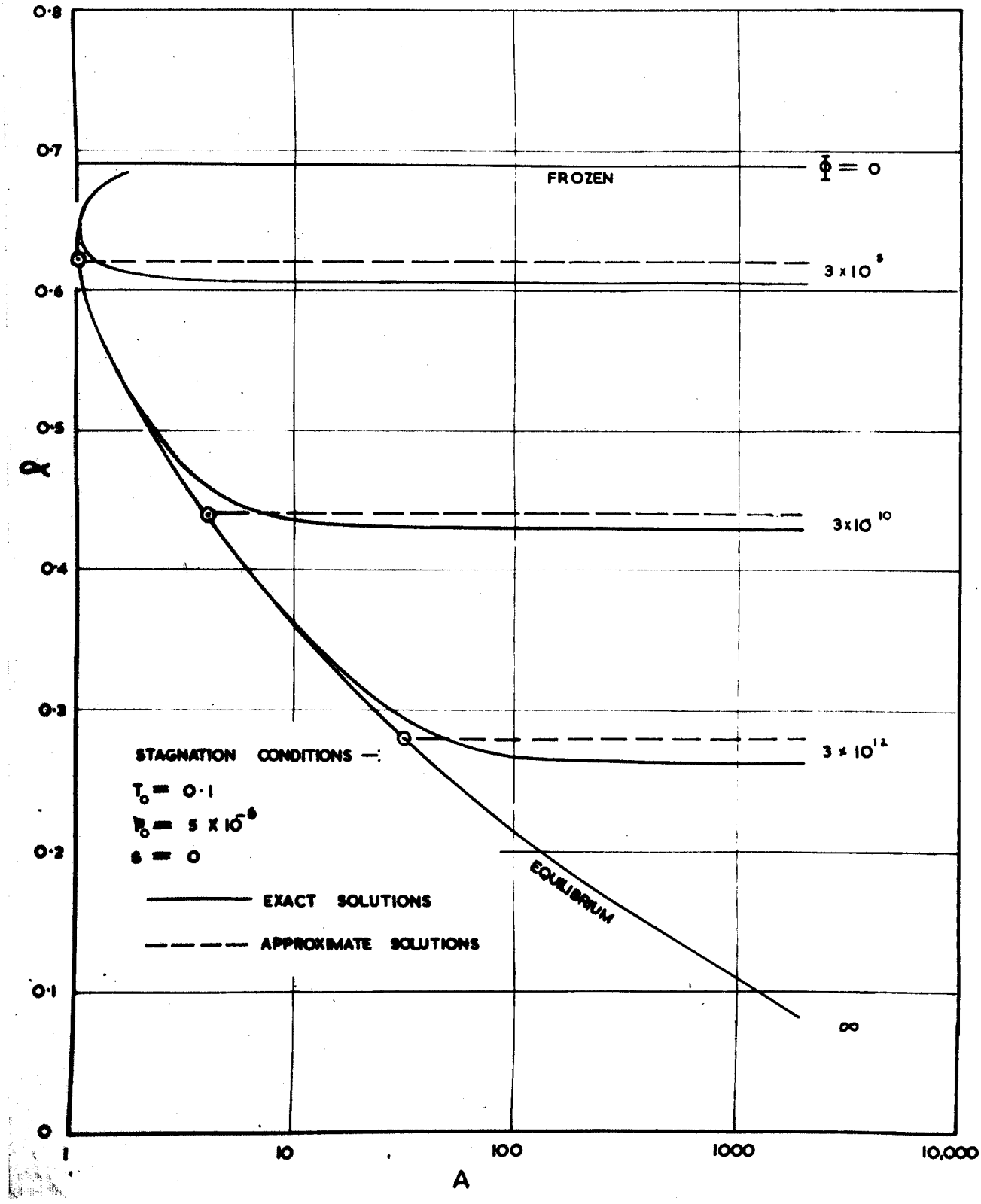

FIG.2 Dissociation fraction

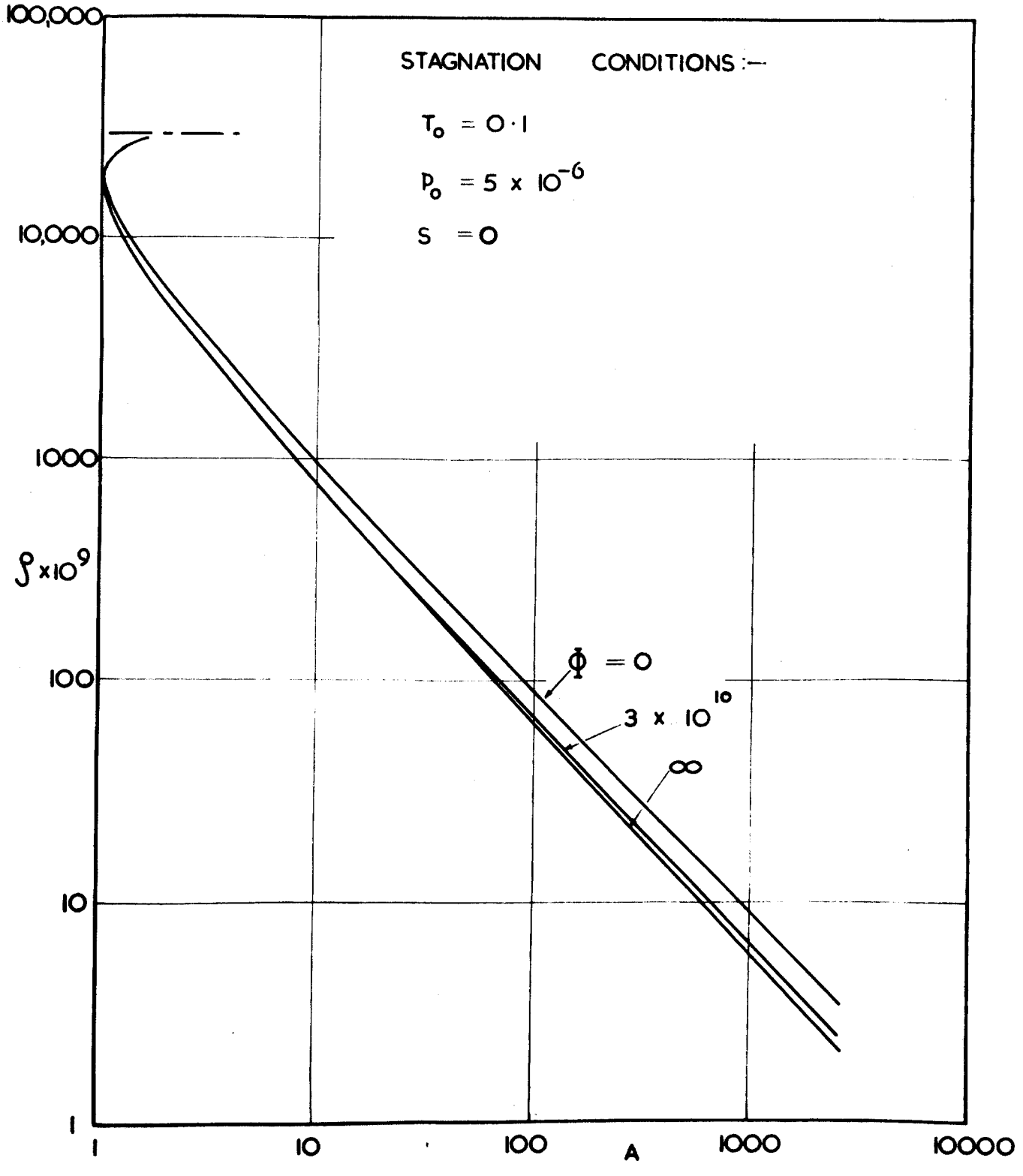

FIG.3 Reduced density

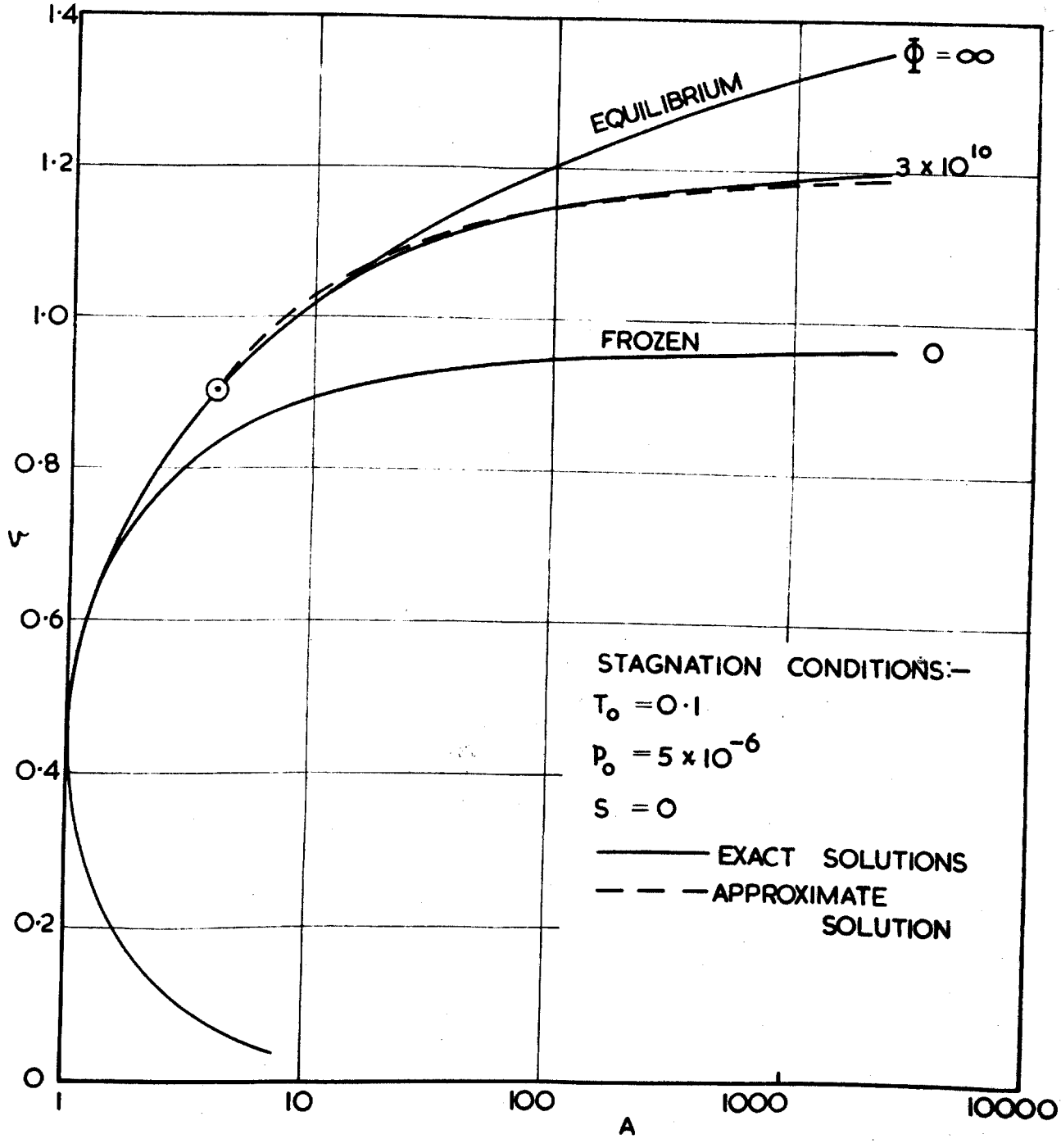

FIG.4 Reduced velocity.

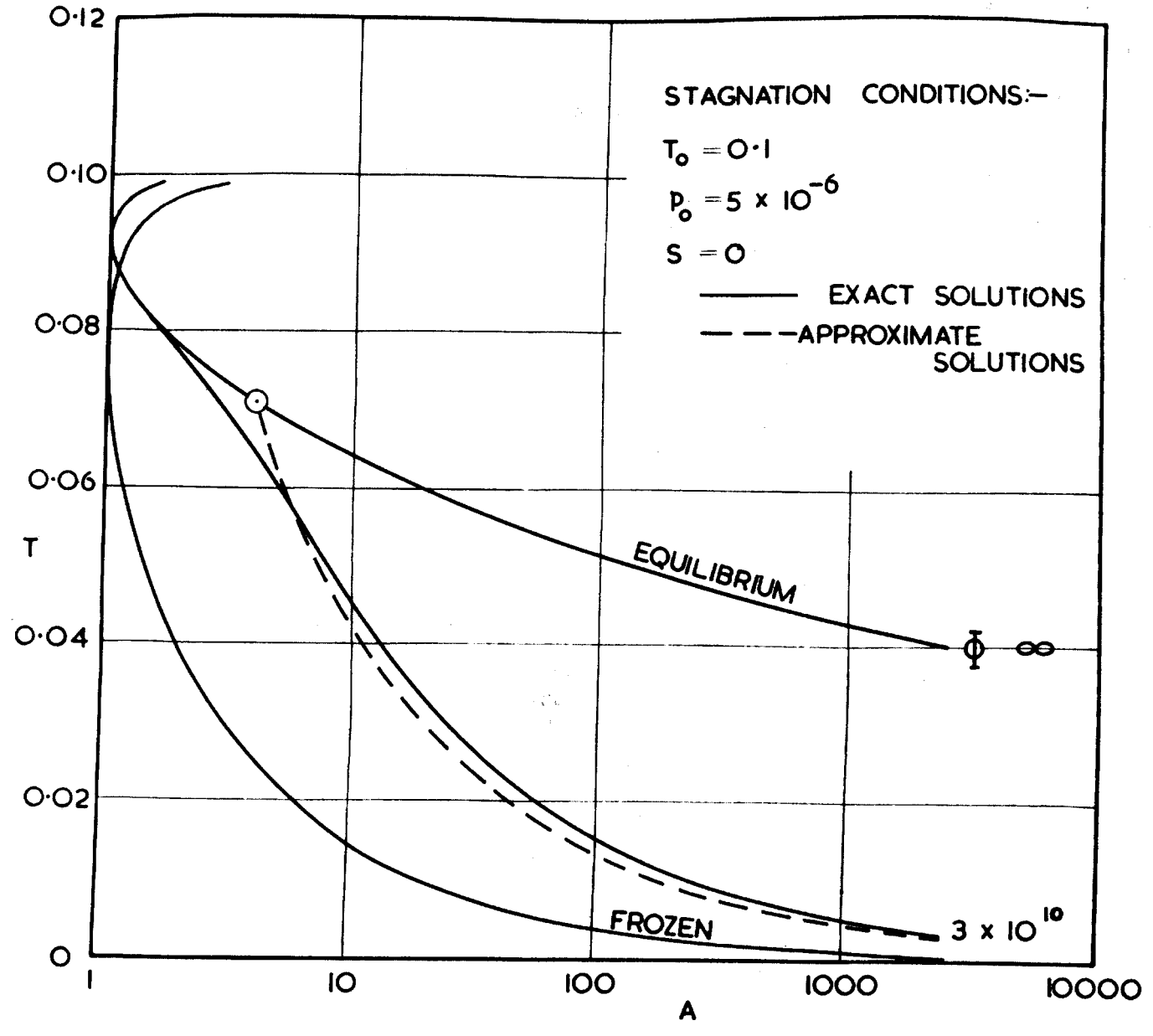

FIG.5 Reduced temperature.

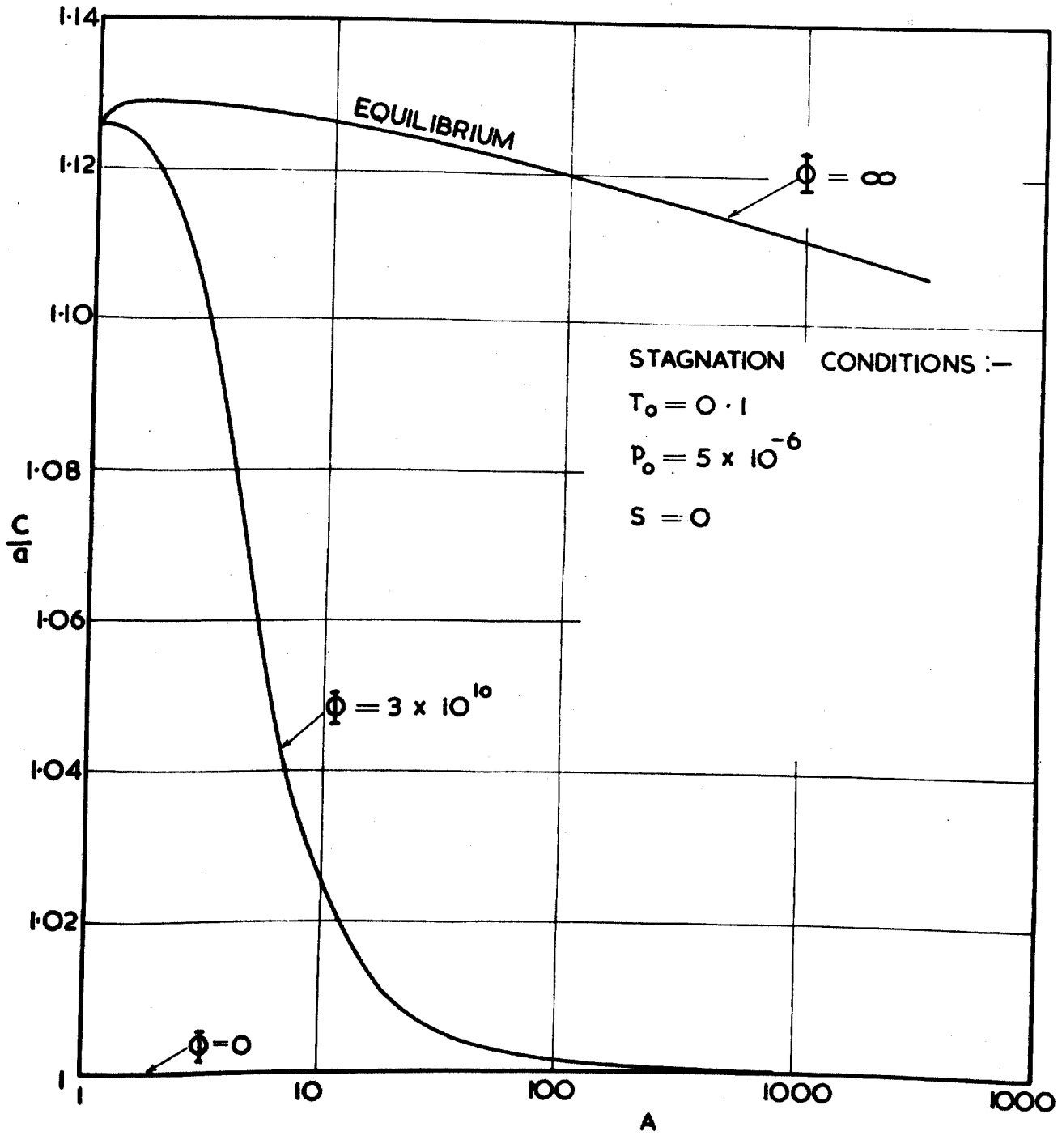

FIG.6 The ratio of characteristic speed to sound speed.

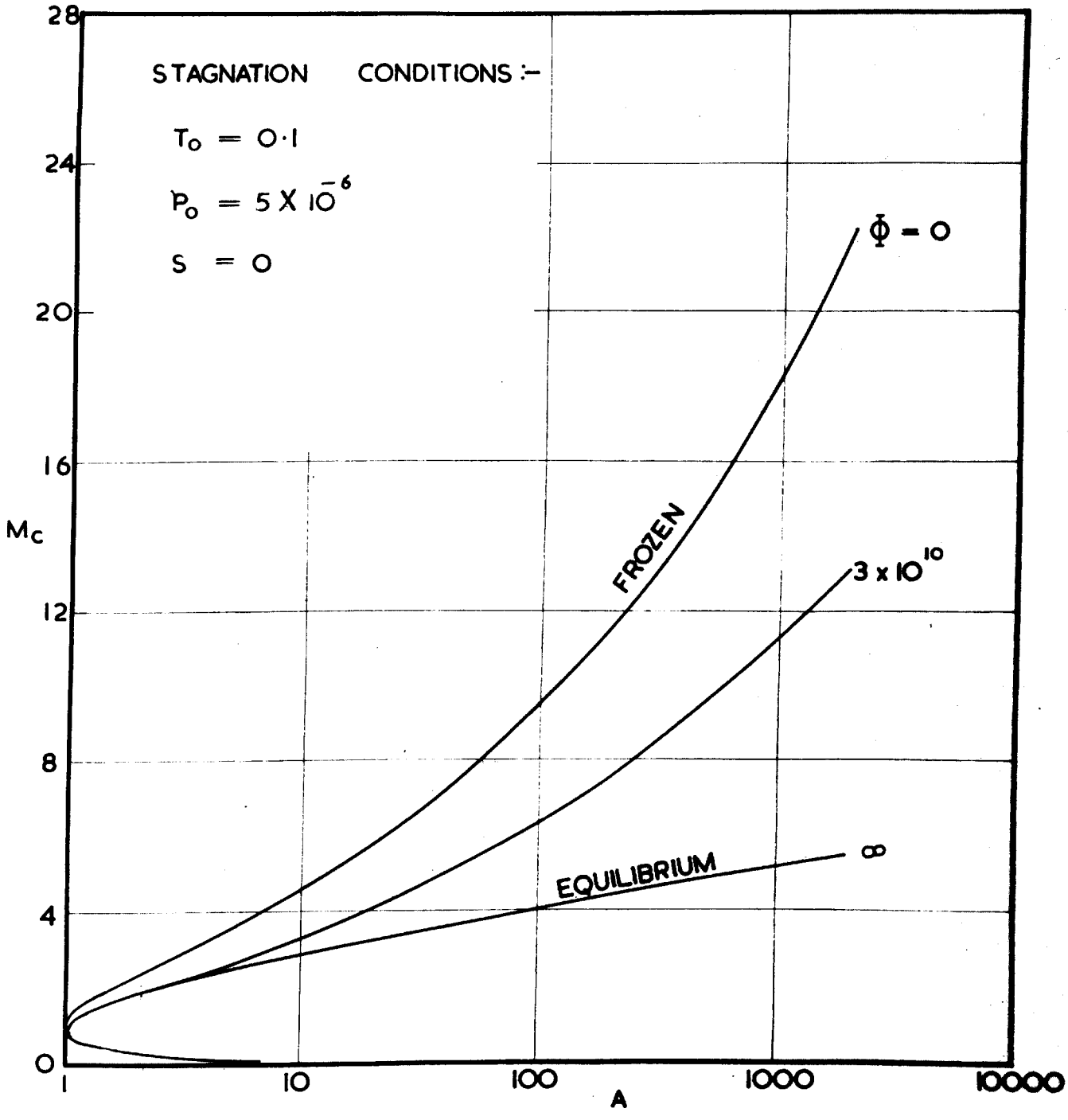

FIG.7 Mach number.

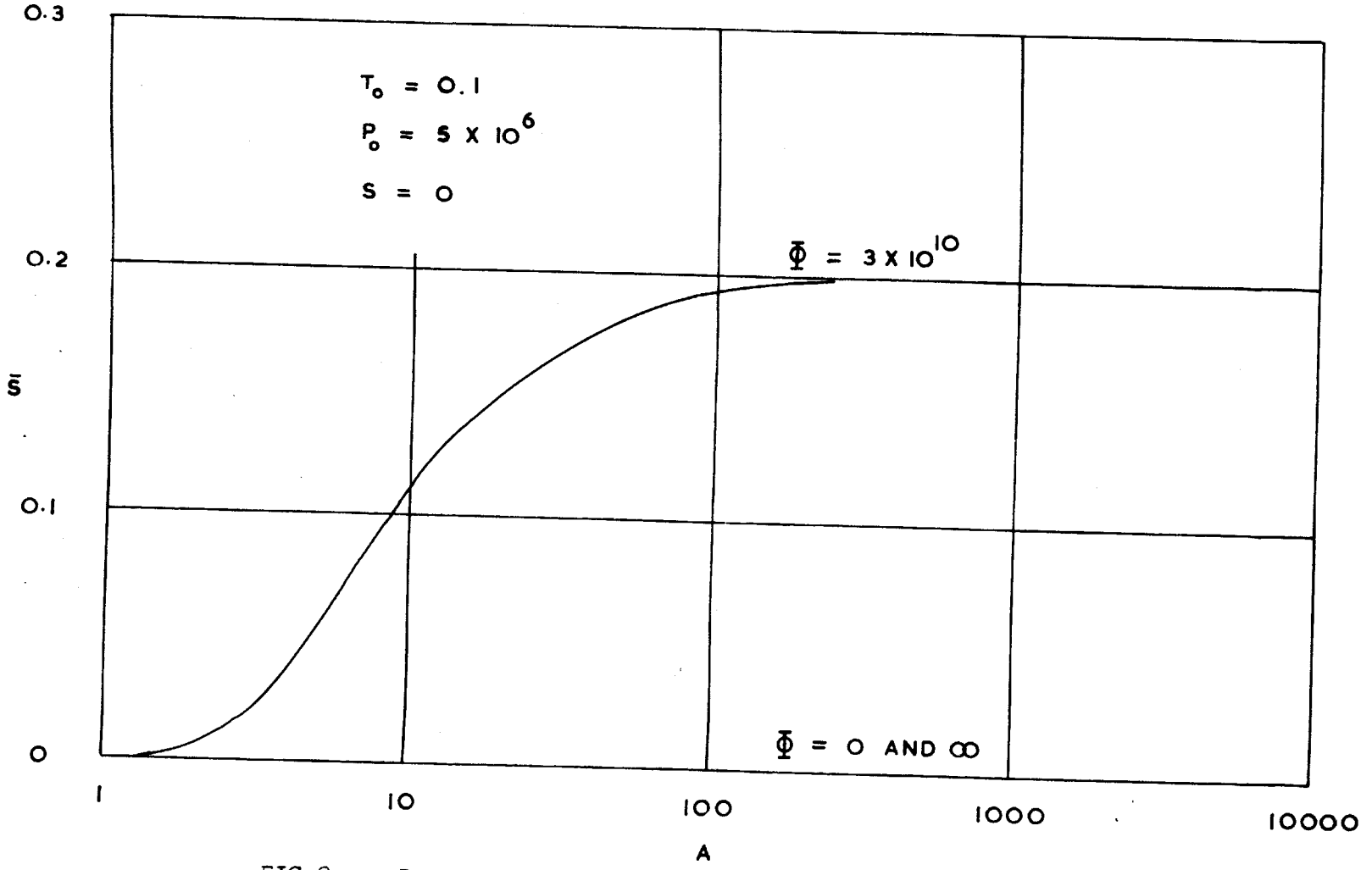

FIG.8 Reduced specific entropy.

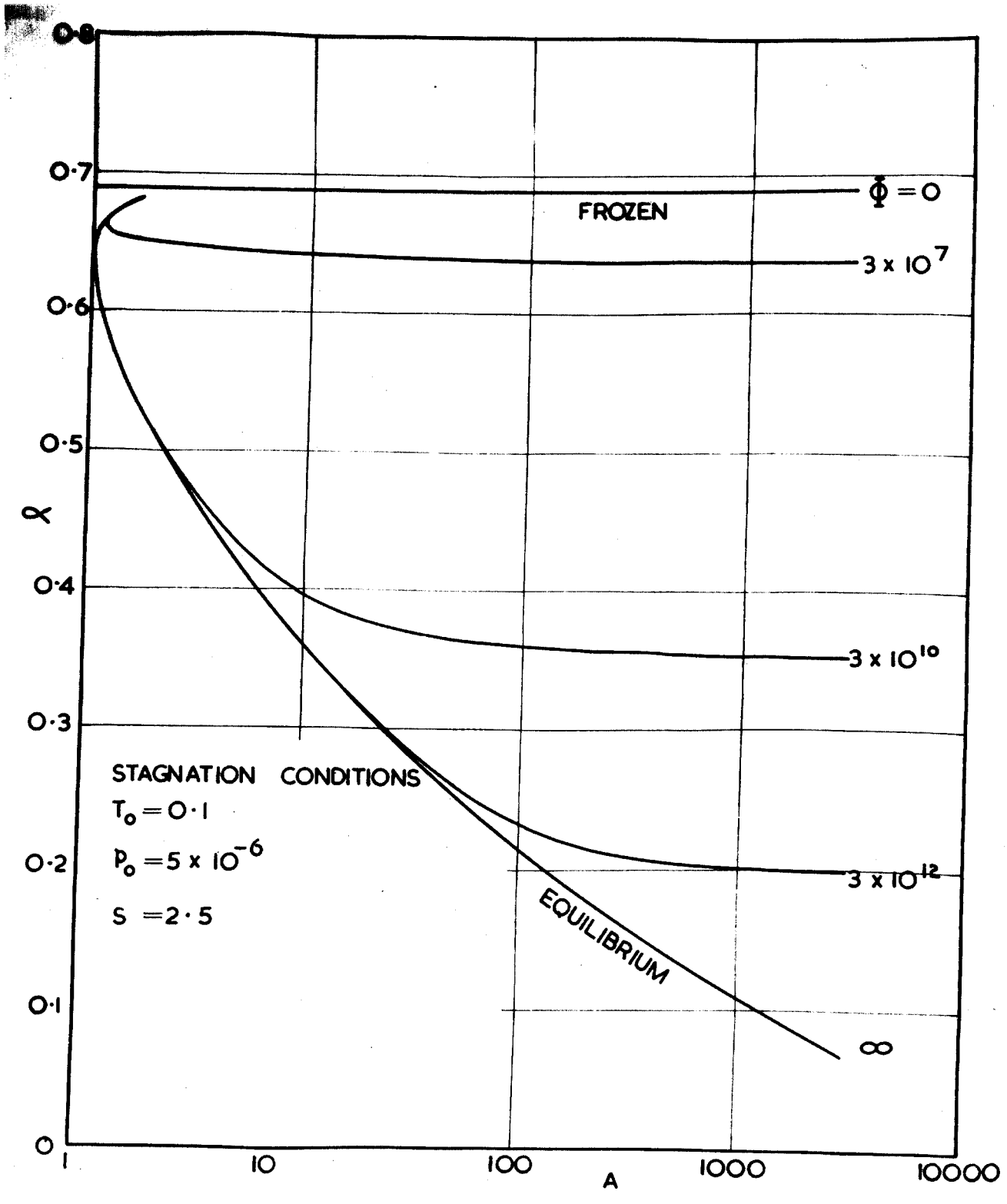

FIG.9 Dissociation fraction: effect of s = 2·5

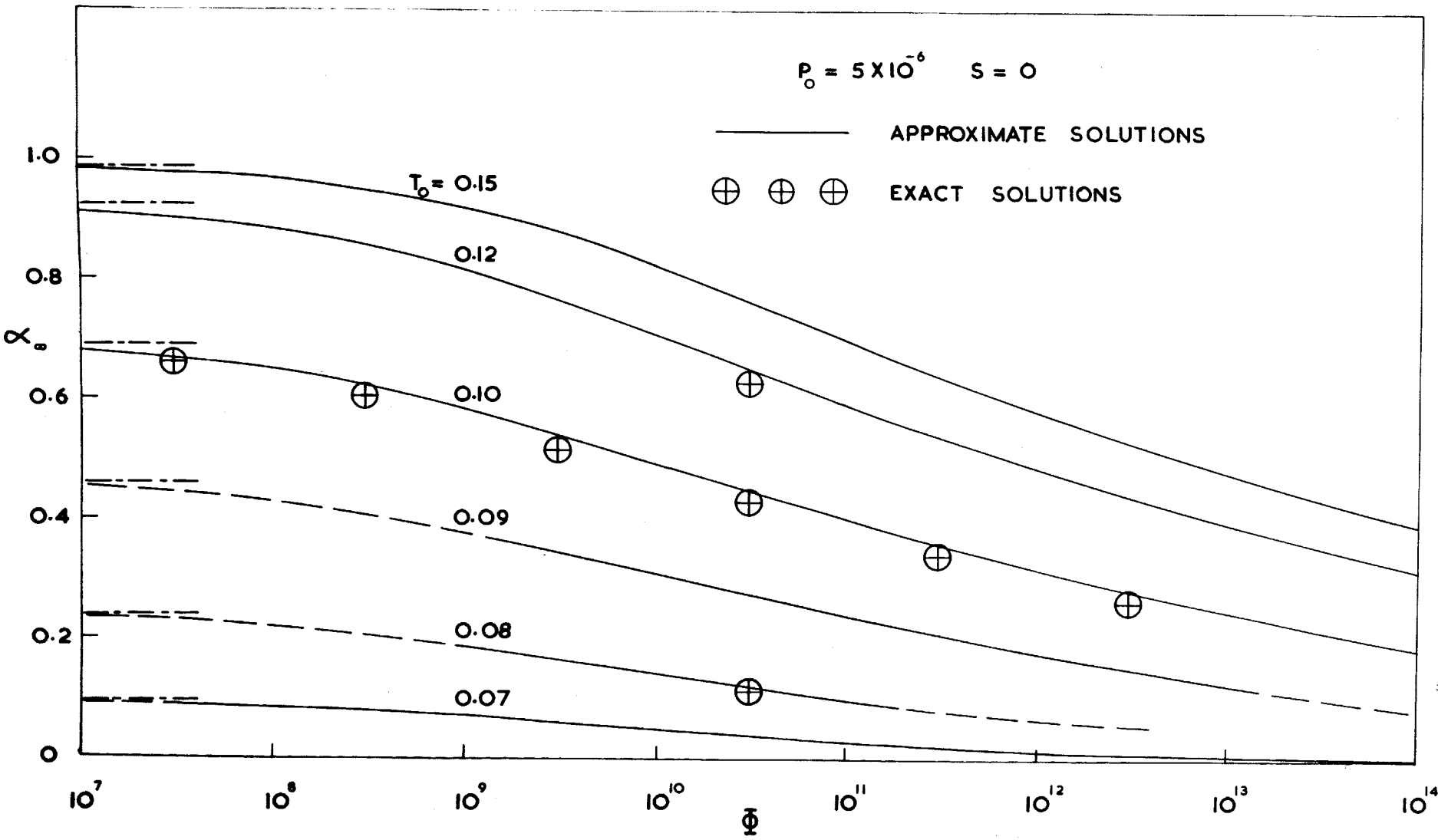

FIG.10 Limiting value of dissociation fraction - effect of temperature.

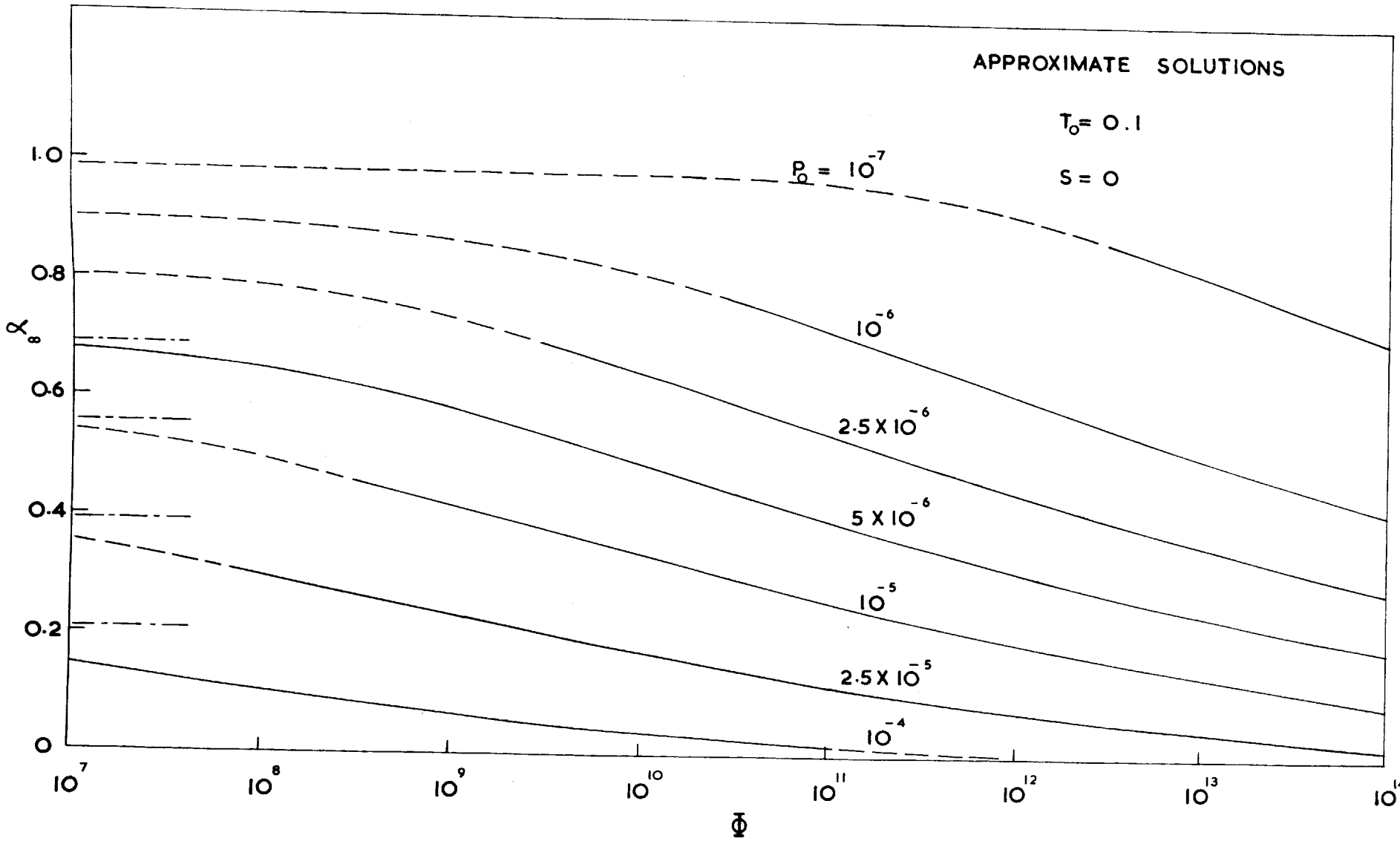

FIG.11 Limiting value of dissociation fraction - effect of pressure.

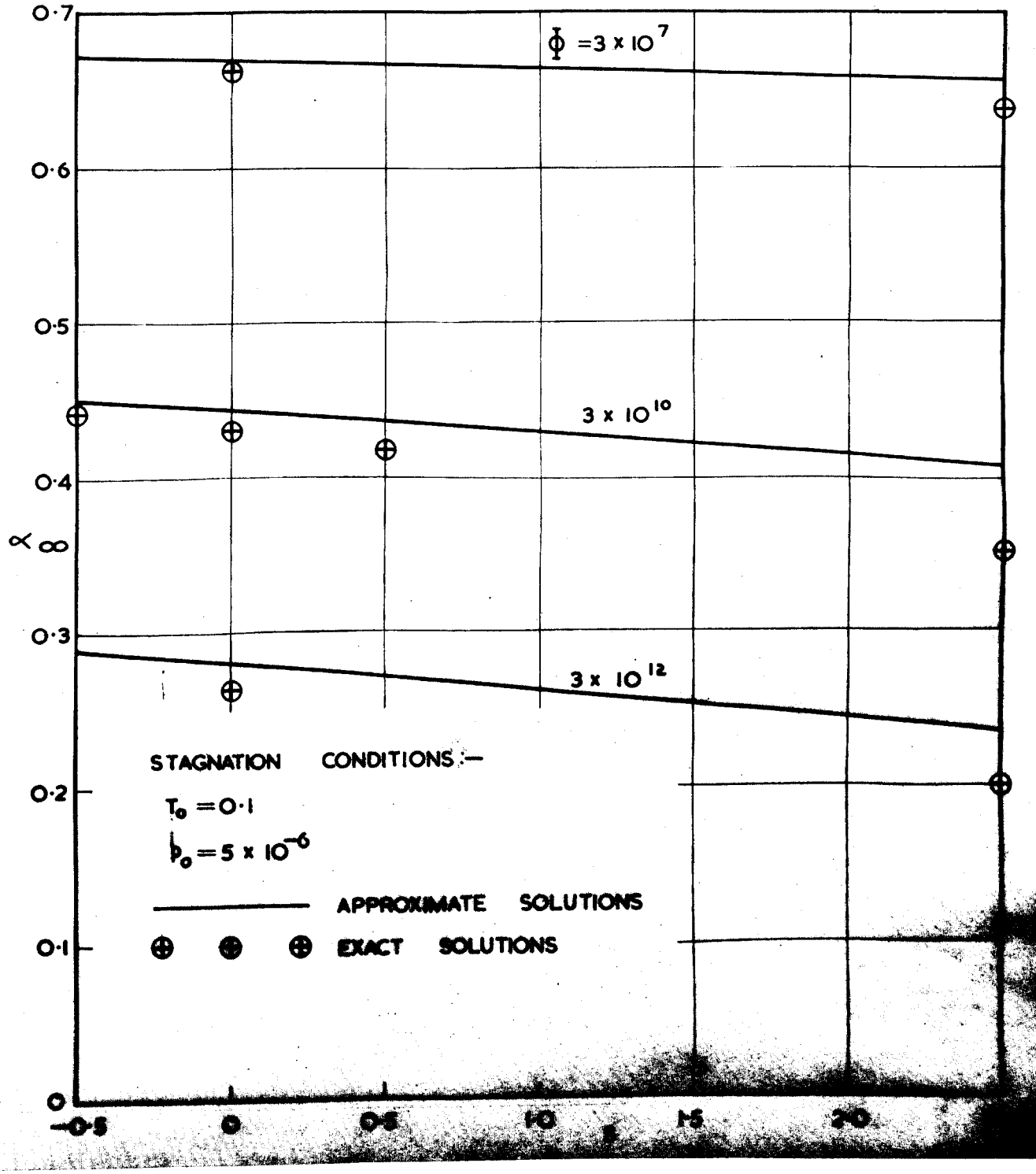

FIG.12 Limiting value of dissociation fraction - Effect of s.

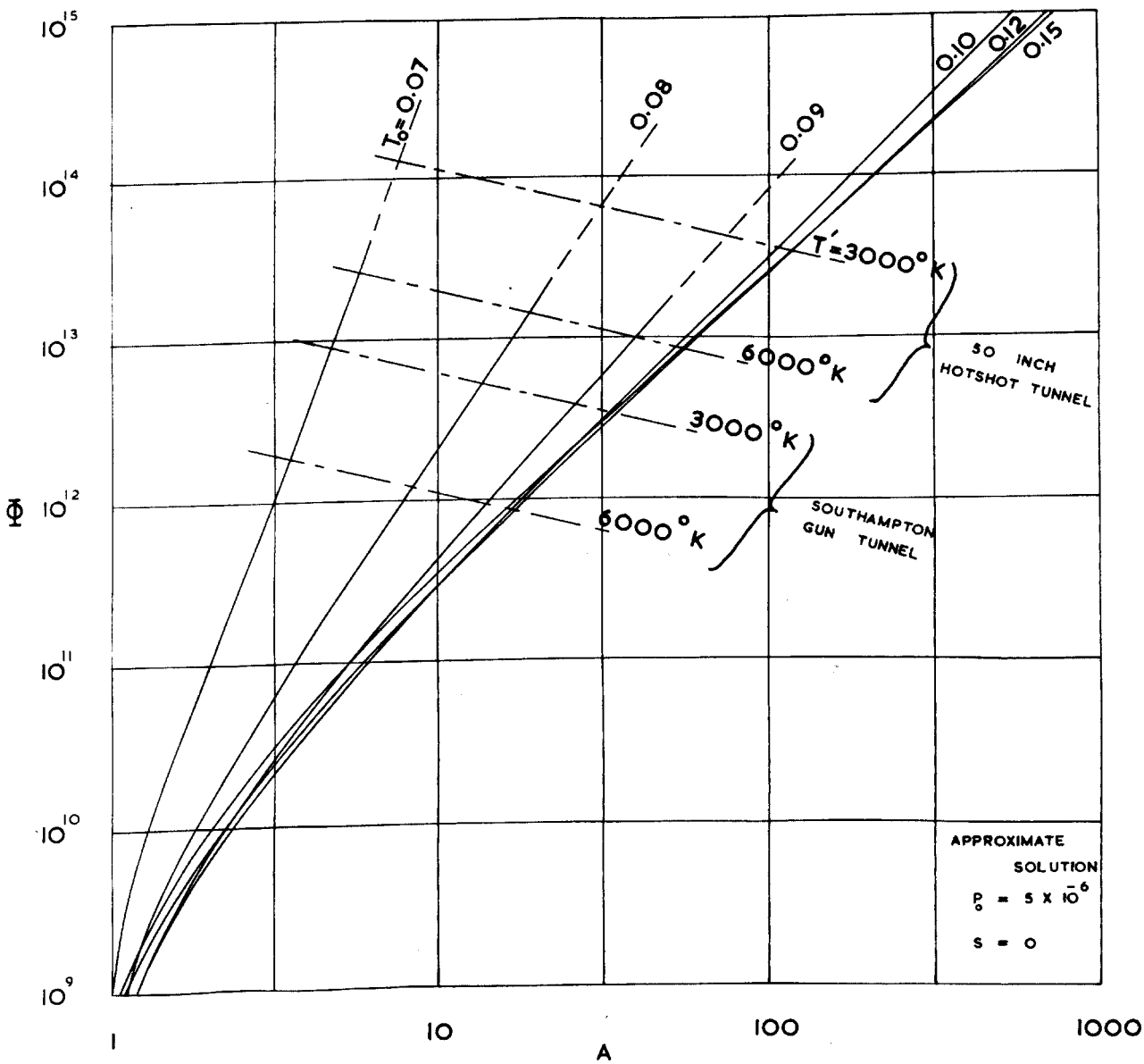

FIG.13 Rate parameter and area ratio for sudden freezing - effect of temperature.

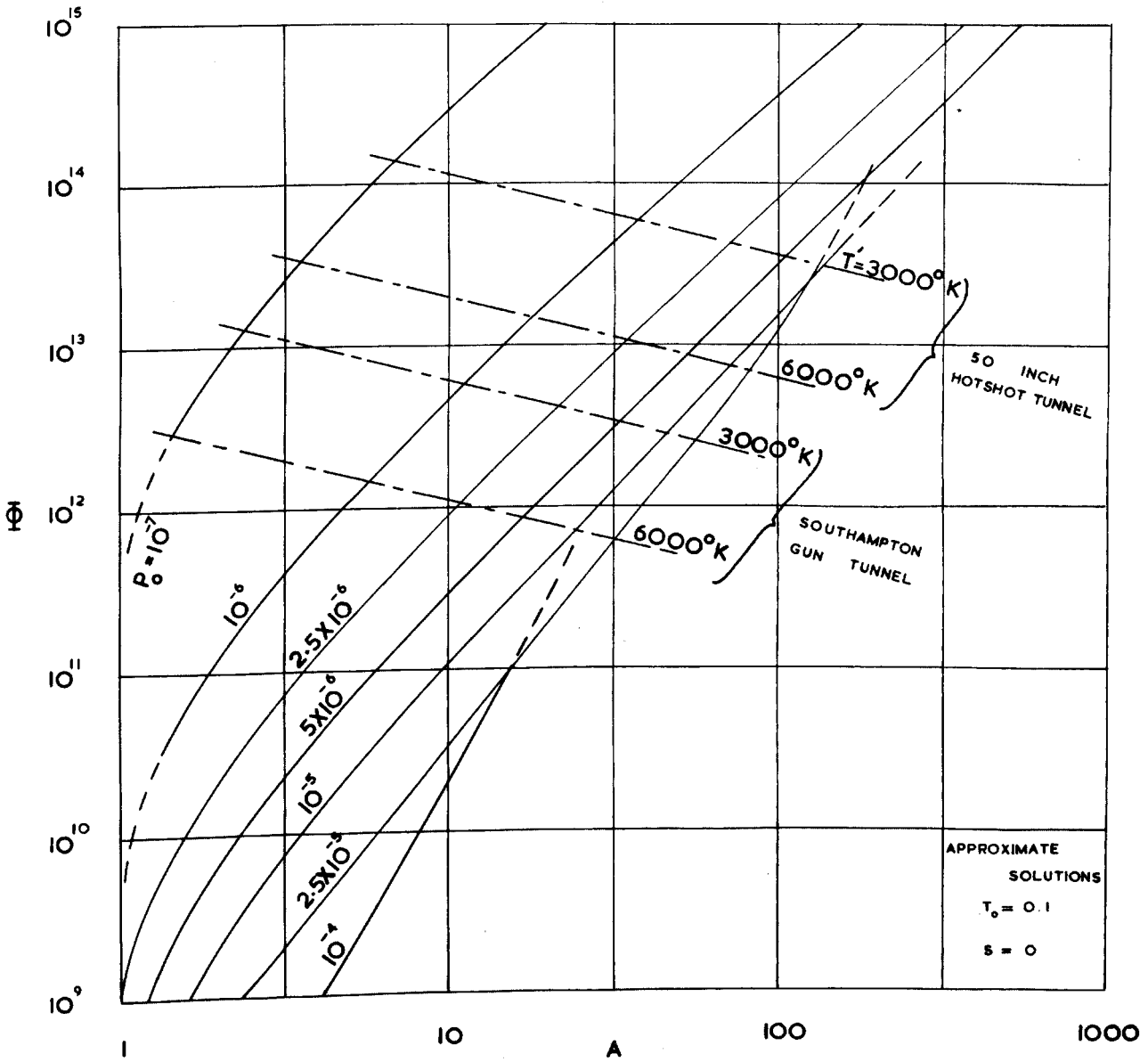

FIG.14 Rate parameter and area ratio for sudden freezing - effect of pressure.

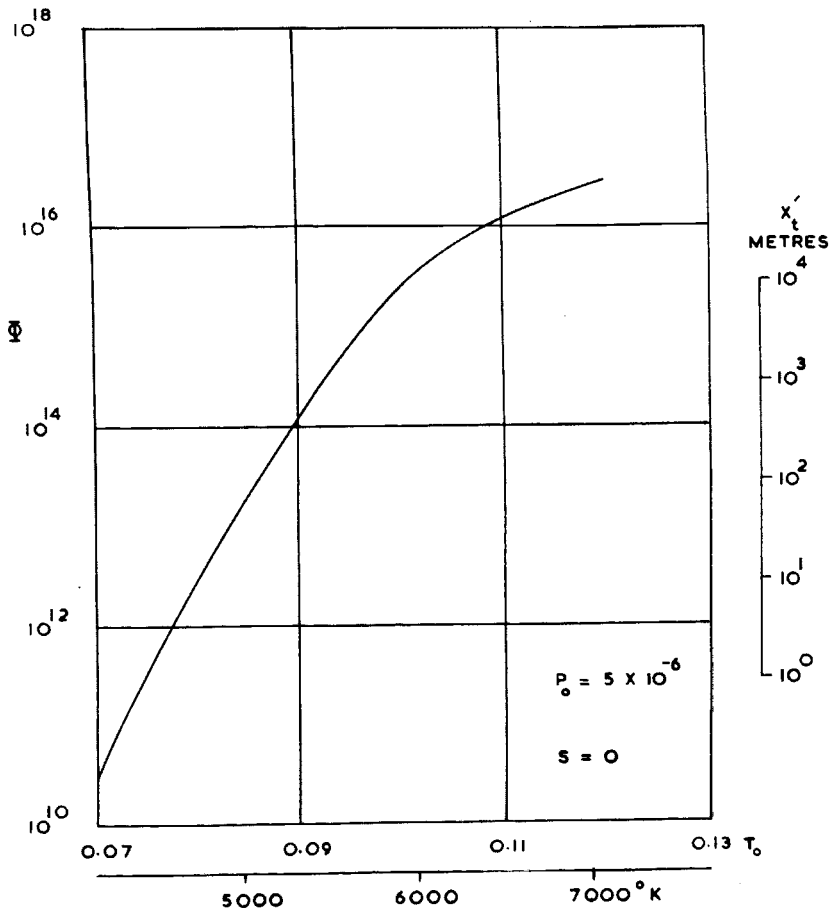

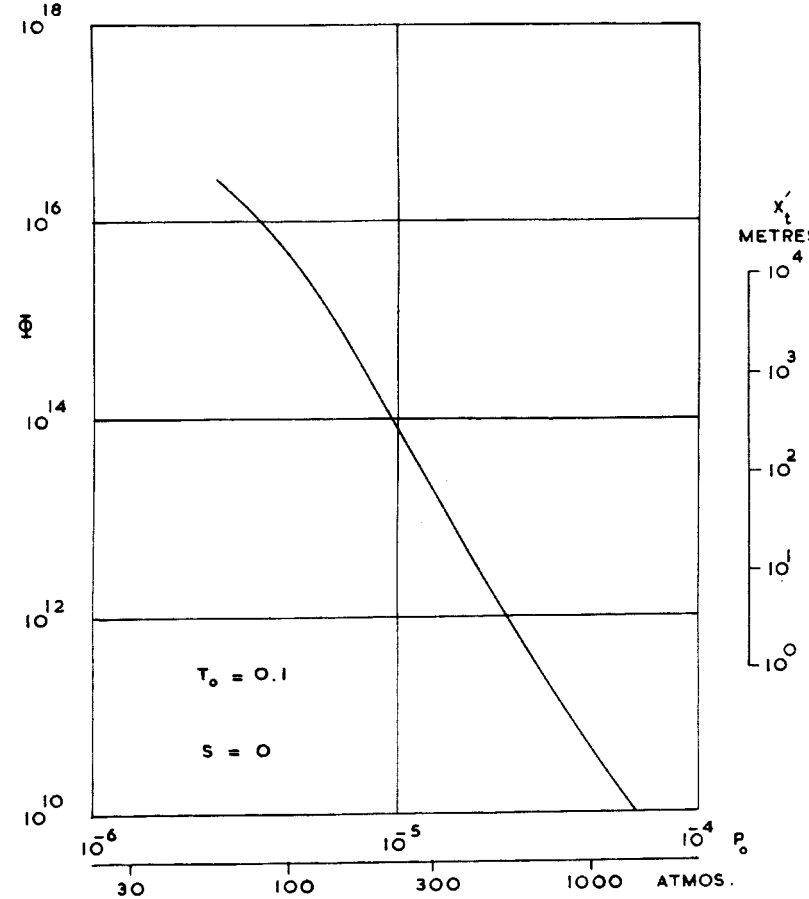

FIGS.15 and 16 Values of rate parameter so that 10% of total energy is frozen in dissociation: Dimensional values are for oxygen, using rate constant of Mathews (1959), matched at 6,000°K.

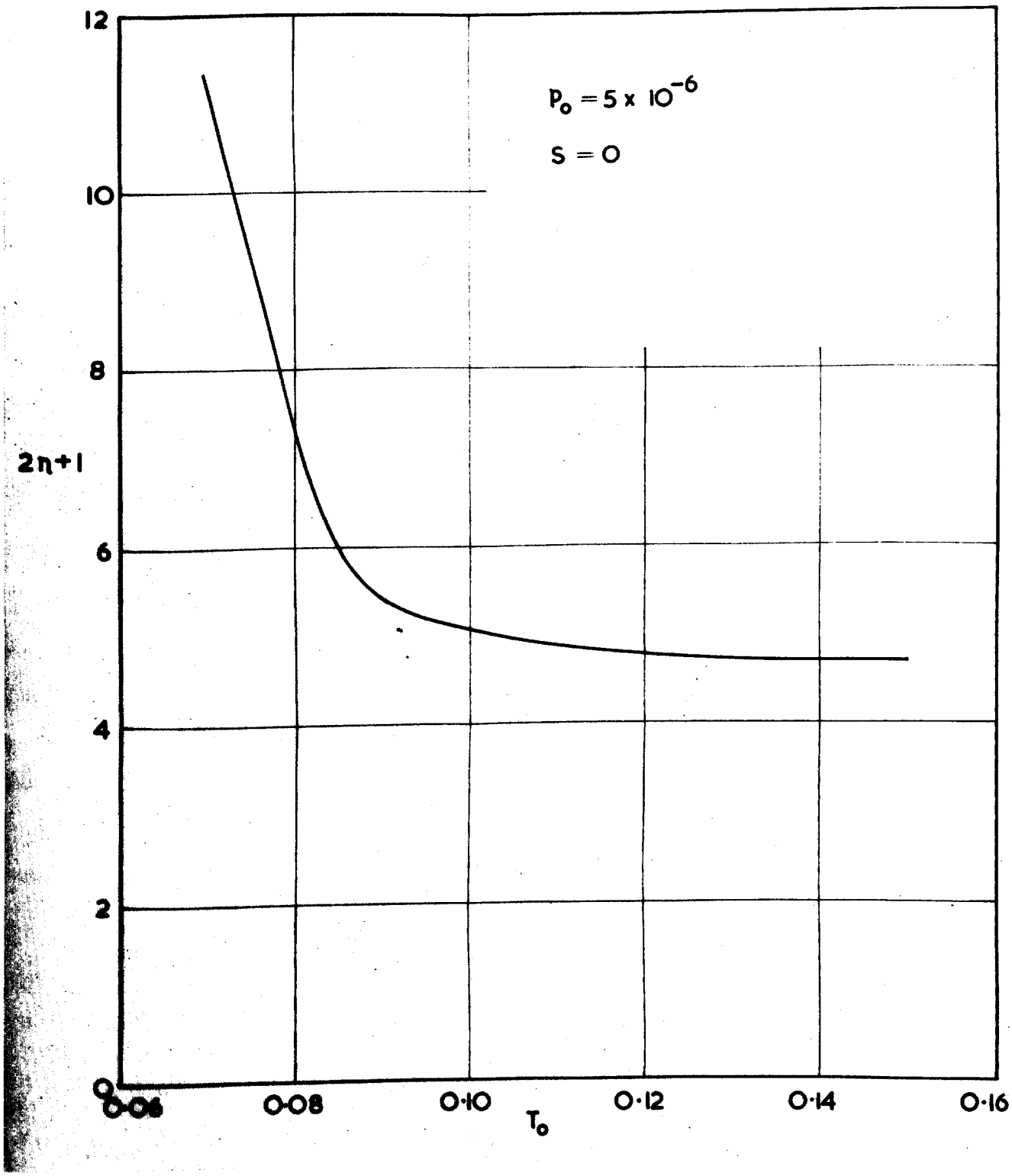

FIG.17 Ratio of length of conical nozzle to length of corresponding optimum nozzle.

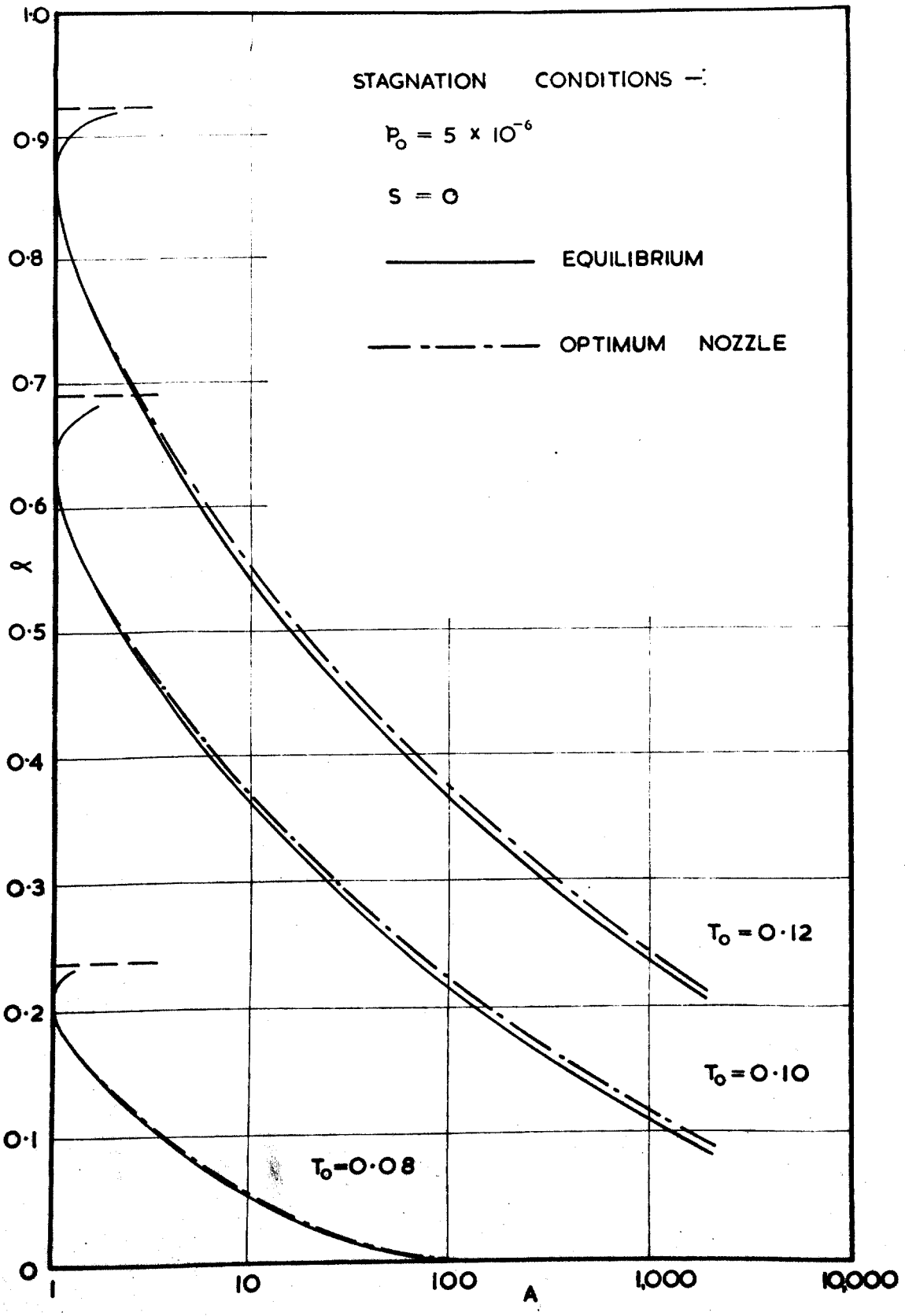

FIG.18 Dissociation fraction for optimum nozzles.

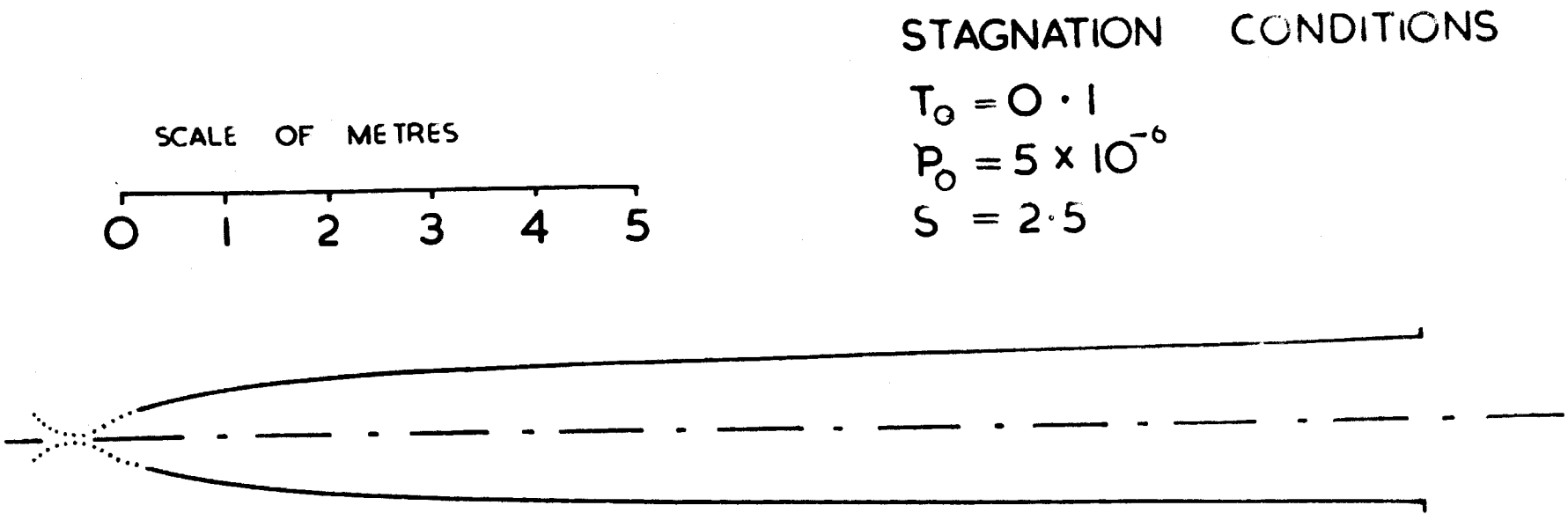

FIG.19 Shape of optimum nozzle using Mathews' rate constant matched at 3,000°K.

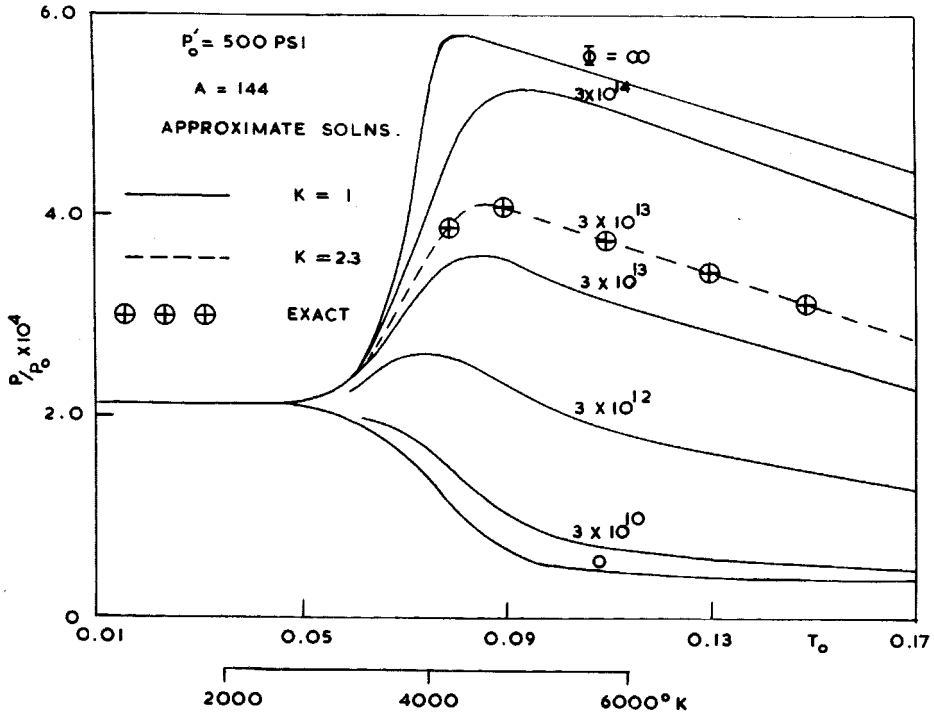

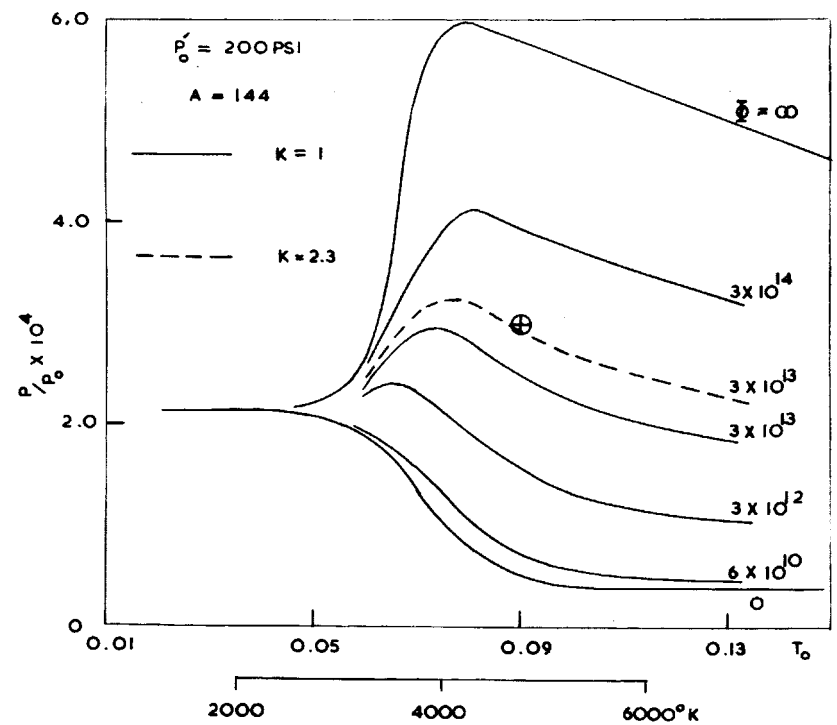

FIGS.20 and 21 Pressure ratio versus temperature. Calculations for oxygen.

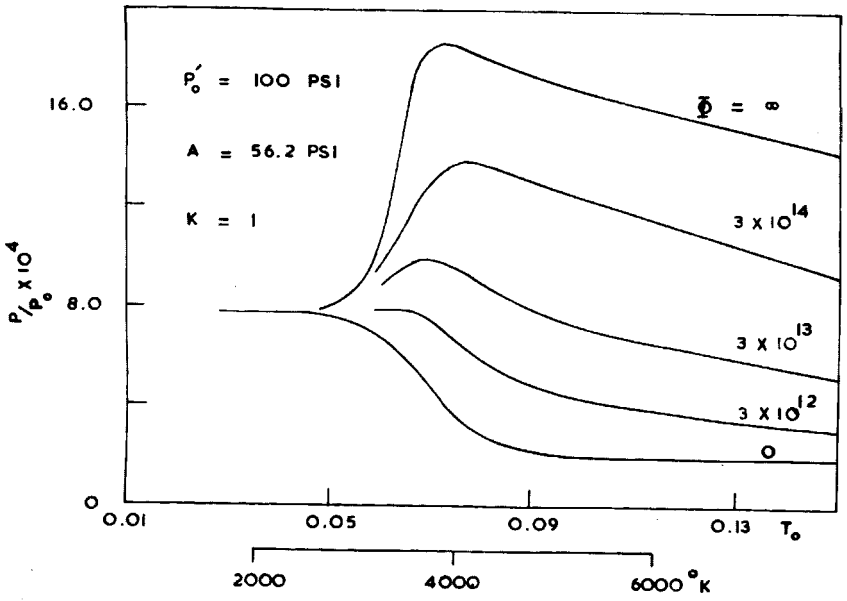

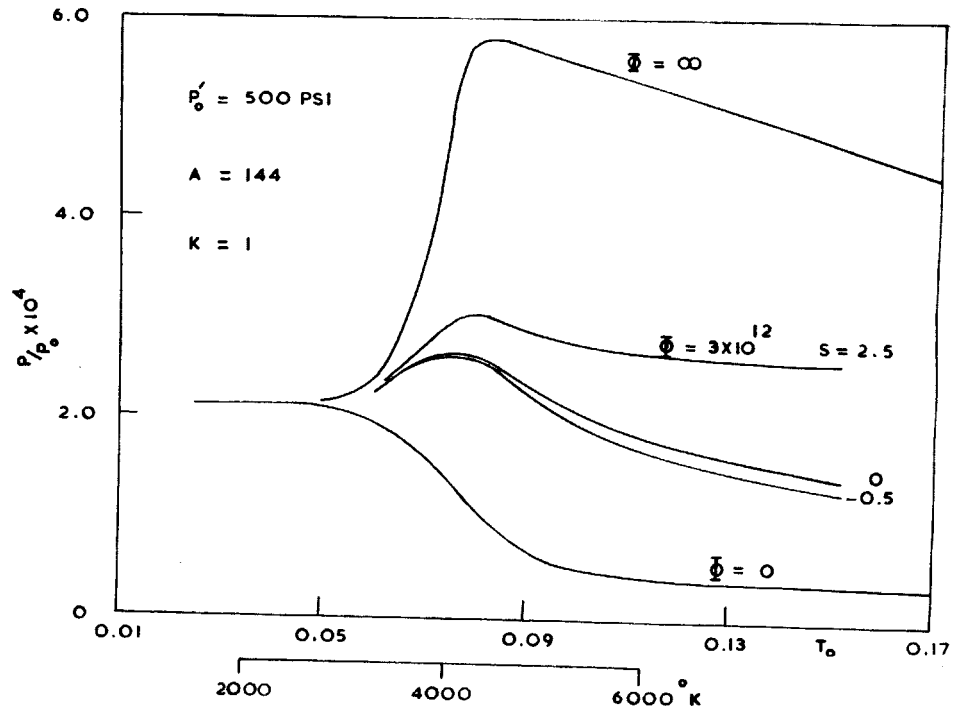

FIGS.22 and 23 Pressure ratio versus temperature. Calculations for oxygen.

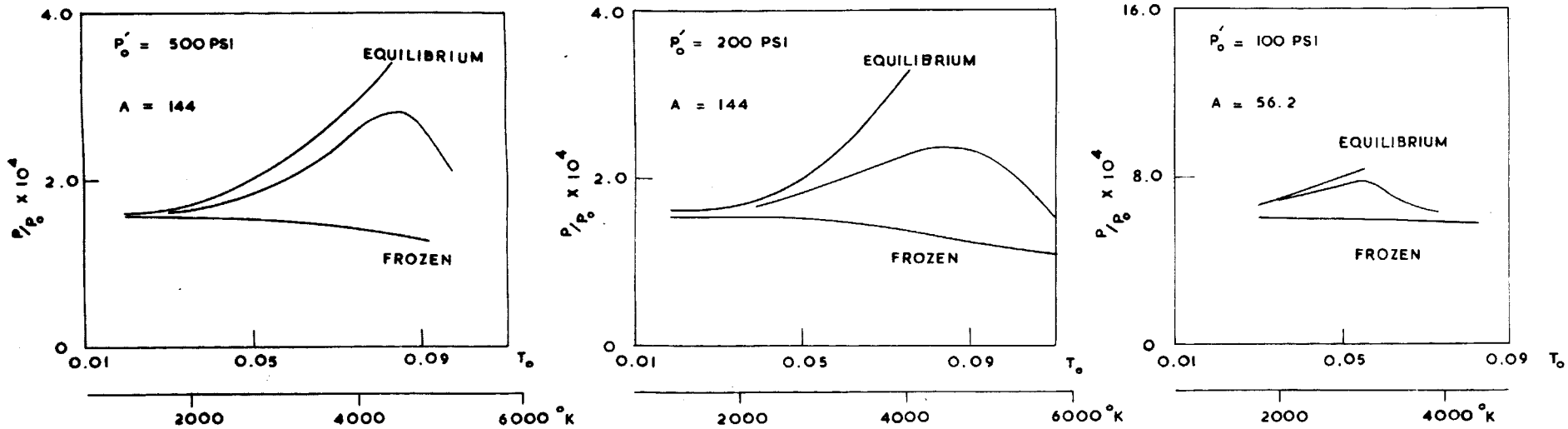

FIGS. 24, 25 and 26 Pressure ratio versus temperature: G.E.C. experiments on air.

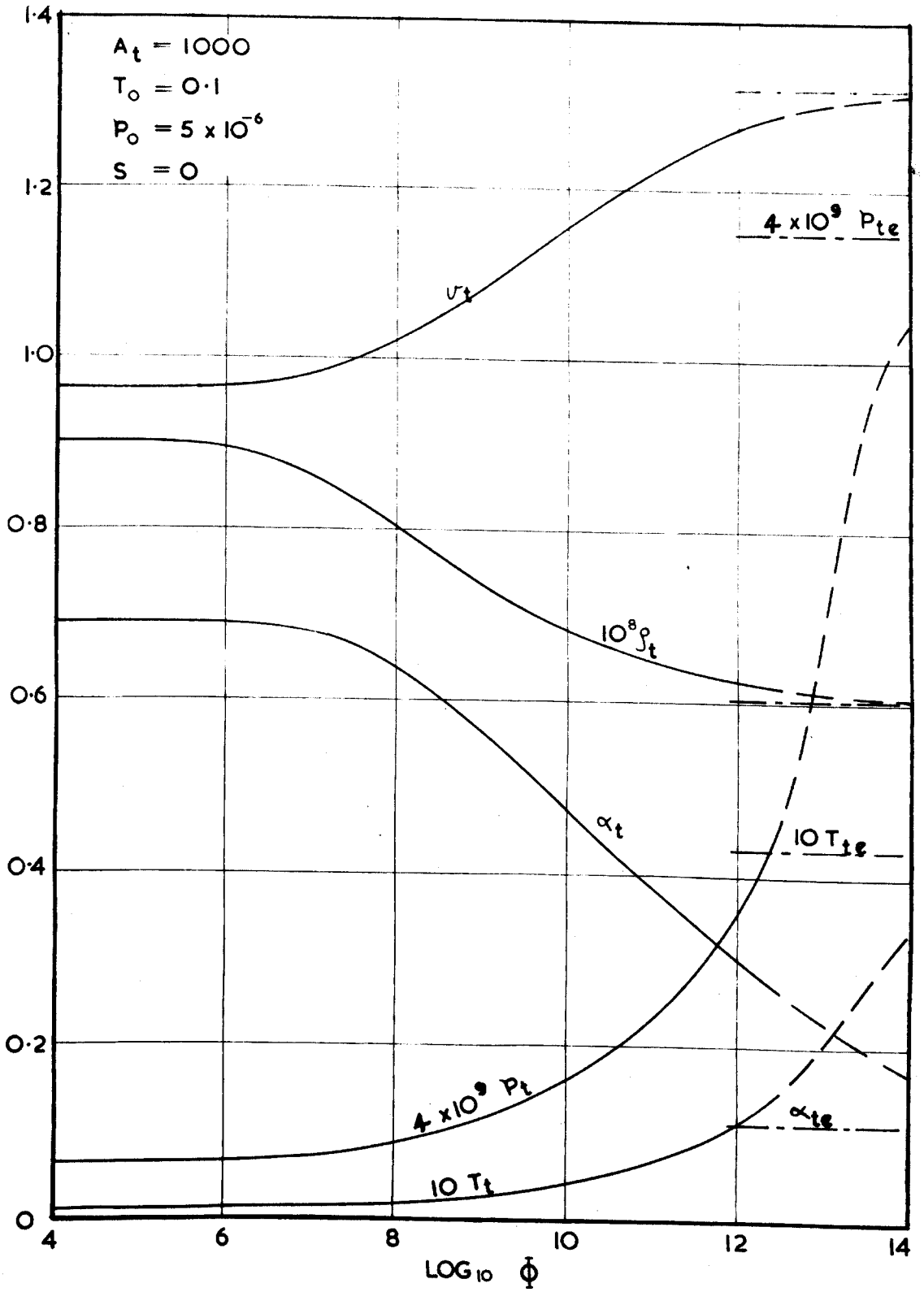

FIG.27 Test section conditions.

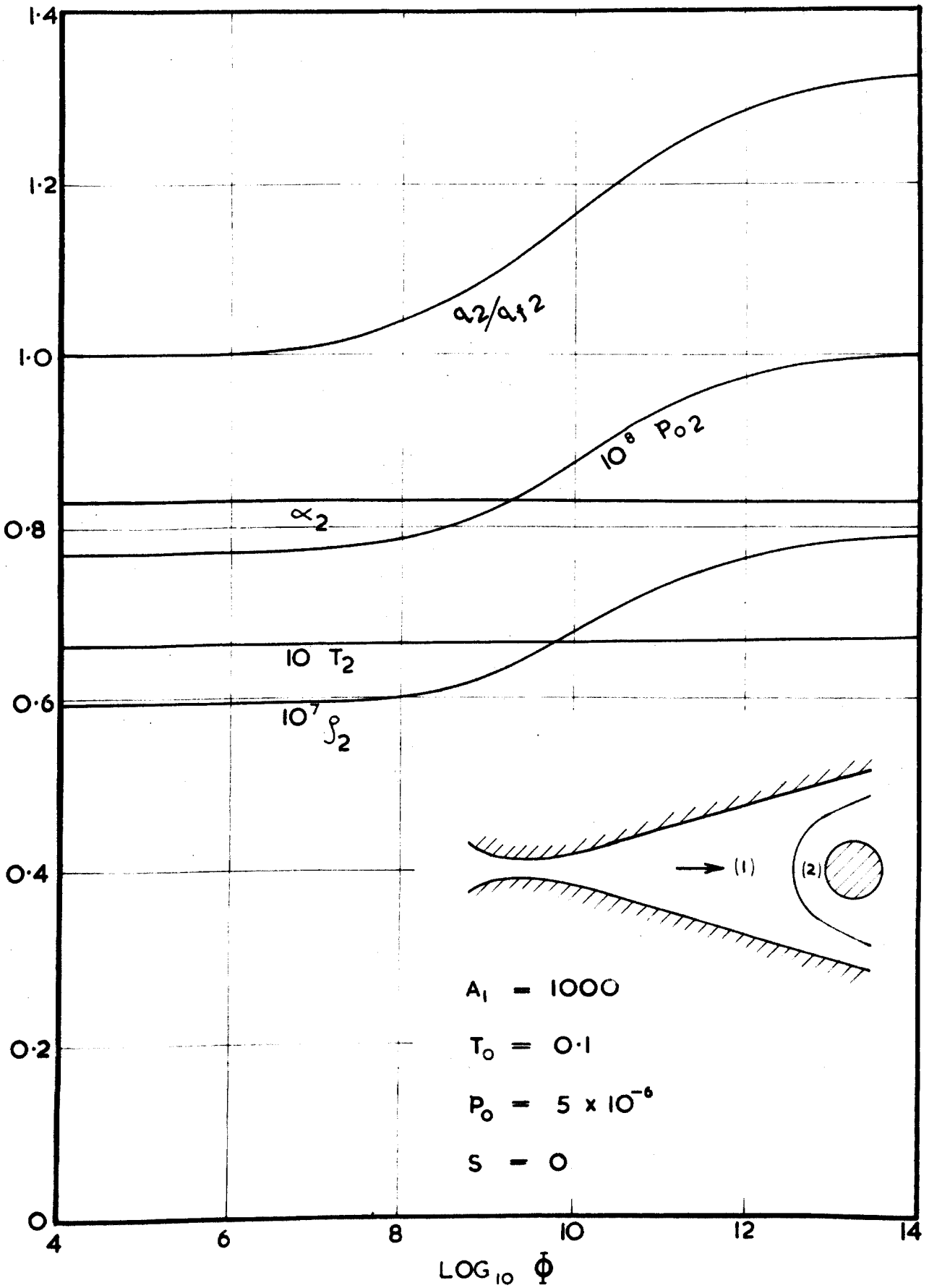

FIG.28 Conditions behind a normal shock wave.

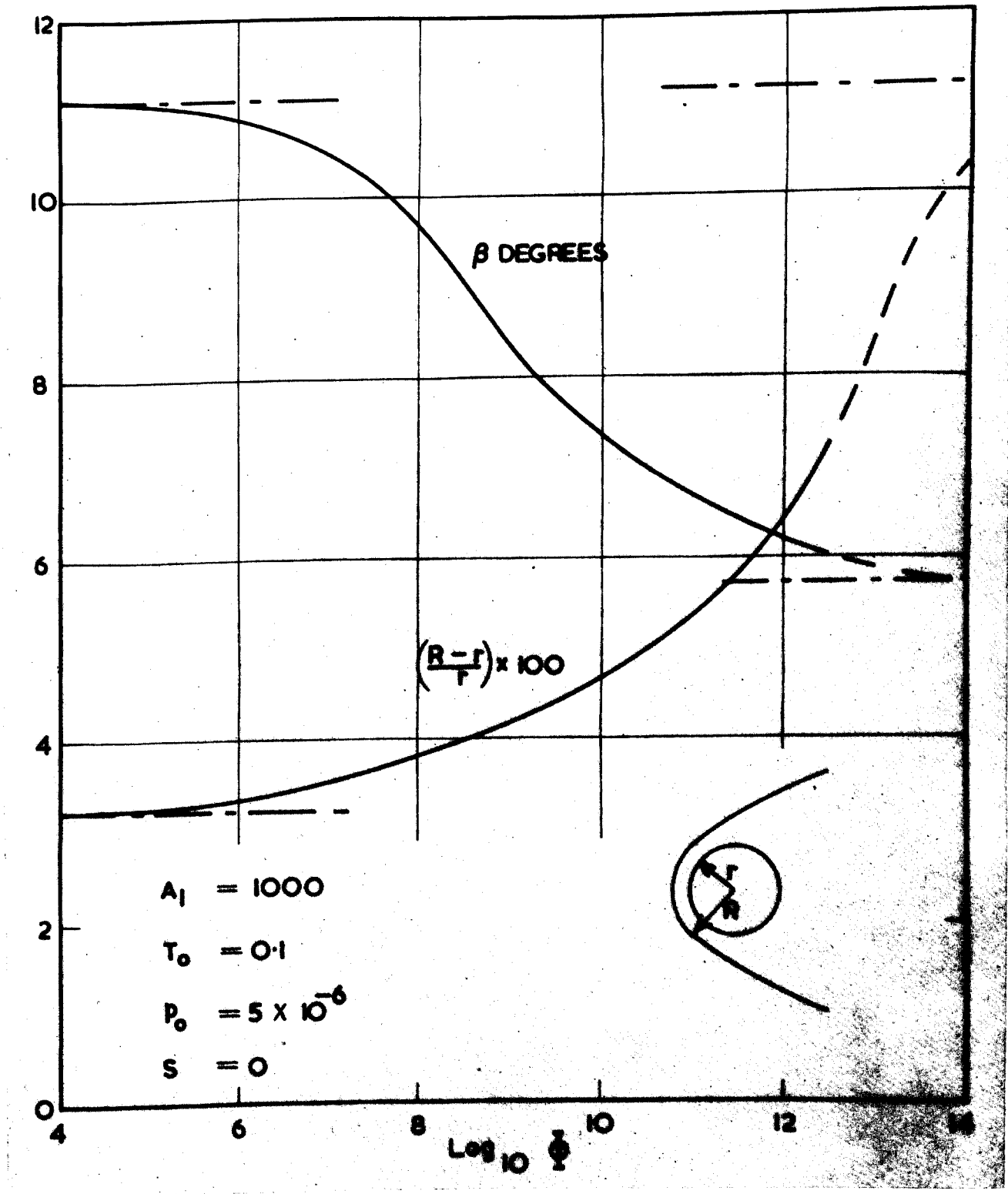

FIG.29 Mach angle and stand-off distance for a sphere.

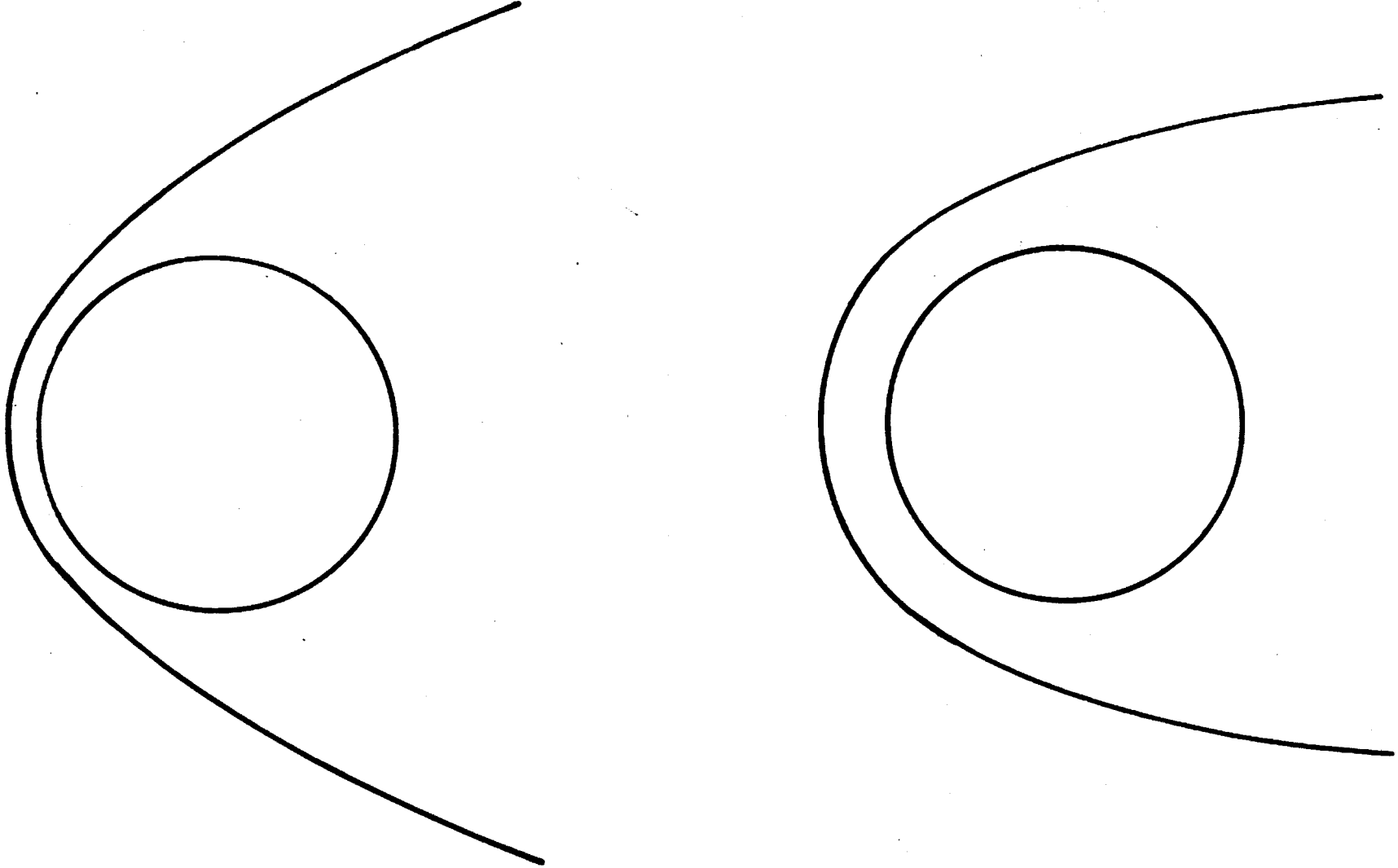

FIG.30 Shock wave shapes for equilibrium and frozen flow (not to scale).

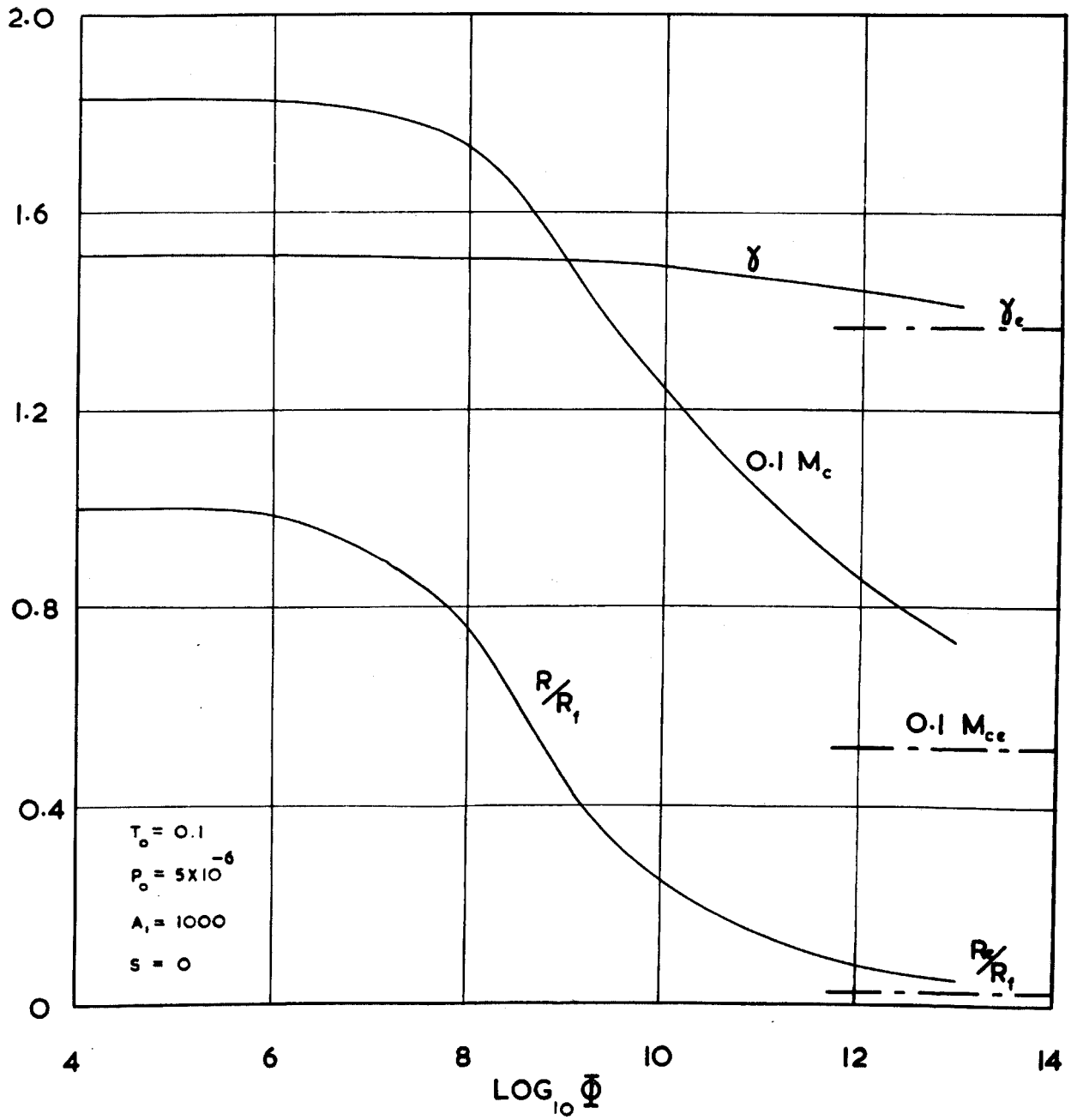

FIG.31 Some test section parameters affecting flow past a slender body.